
ROBUST-MULTI-TASK GRADIENT BOOSTING *

Seyedsaman Emami
 Escuela Politécnica Superior
 Universidad Autónoma de Madrid
 Madrid

Gonzalo Martínez-Muñoz
 Escuela Politécnica Superior
 Universidad Autónoma de Madrid
 Madrid

Daniel Hernández-Lobato
 Escuela Politécnica Superior
 Universidad Autónoma de Madrid
 Madrid

ABSTRACT

Multi-task learning (MTL) has shown effectiveness in exploiting shared information across tasks to improve generalization. MTL assumes tasks share similarities that can improve performance. In addition, boosting algorithms have demonstrated exceptional performance across diverse learning problems, primarily due to their ability to focus on hard-to-learn instances and iteratively reduce residual errors. This makes them a promising approach for learning multi-task problems. However, real-world MTL scenarios often involve tasks that are not well-aligned (known as outlier or adversarial tasks), which do not share beneficial similarities with others and can, in fact, deteriorate the performance of the overall model. To overcome this challenge, we propose Robust-Multi-Task Gradient Boosting (R-MTGB), a novel boosting framework that explicitly models and adapts to task heterogeneity during training. R-MTGB structures the learning process into three sequential blocks: (1) learning shared patterns, (2) partitioning tasks into outliers and non-outliers with regularized parameters, and (3) fine-tuning task-specific predictors. This architecture enables R-MTGB to automatically detect and penalize outlier tasks while promoting effective knowledge transfer among related tasks. Our method integrates these mechanisms seamlessly within gradient boosting, allowing robust handling of noisy or adversarial tasks without sacrificing accuracy. Extensive experiments on both synthetic benchmarks and real-world datasets demonstrate that our approach successfully isolates outliers, transfers knowledge, and consistently reduces prediction errors for each task individually, and achieves overall performance gains across all tasks. These results highlight robustness, adaptability, and reliable convergence of R-MTGB in challenging MTL environments.

Keywords Multi-Task Learning · Gradient Boosting · Outlier Detection · Noise-Aware Modeling

*This manuscript is currently under review at *Neurocomputing*.

List of Abbreviations

CD	Critical Distance
DP	Data Pooling
DTR	Decision Tree Regressor
GB	Gradient Boosting
MAE	Mean Absolute Error
ML	Machine Learning
MTGB	Multi-Task Gradient Boosting
MTL	Multi-Task Learning
R-MTGB	Robust-Multi-Task Gradient Boosting
RMSE	Root Mean Squared Error
ST	Single Task
TaF	Task as Feature

1 Introduction

Machine Learning (**ML**) models are increasingly used in scenarios that require learning multiple prediction tasks at the same time. This approach, referred to as Multi-Task Learning (**MTL**), which involves learning multiple related or unrelated tasks simultaneously by transferring knowledge from one task to another [1]. The main objective of **MTL** is to improve generalization performance by utilizing task-specific information and leveraging shared representations across tasks [2]. **MTL** has demonstrated significant potential in areas such as computer vision [3, 4] and healthcare [5, 6]. By exploiting shared structures across tasks, **MTL** often achieves better generalization compared to training separate models for each task. However, practical applications frequently involve noisy, diverse, or even adversarial task environments, which makes robustness an essential consideration. In such cases, conventional **MTL** models can experience substantial performance degradation when some tasks are corrupted, poorly defined, or unrelated to the other tasks at all [7].

Gradient Boosting (**GB**) variants have become one of the most effective techniques in supervised learning, especially when applied with decision trees [8, 9, 10]. Building on this success, Multi-task **GB** extends the **GB** framework to handle multiple related learning tasks simultaneously, by modeling each as a combination of a shared component and a task-specific component. Specifically, each task-function is decomposed into a global function that captures the common structure among tasks, and an individual function that accounts for task-specific deviations [11, 12]. This formulation enables implicit data sharing and acts as a regularizer, improving generalization—particularly when tasks are similar but not identical. Unlike single-task learning, which ignores potential synergies between tasks, or data pooling, which treats all tasks as identical, multi-task boosting leverages shared structure while respecting task heterogeneity. Empirical results have shown that this method consistently outperforms standard boosting approaches in scenarios where tasks are moderately related [13, 14, 12]. However, if certain tasks are outliers or contain significant noise, the shared model may become distorted, potentially degrading overall performance unless properly regularized or weighted.

Crucially, real-world **MTL** scenarios involve, label noise, and task heterogeneity, where some tasks may differ significantly from others and may not share underlying similarities [7, 15]—conditions that often degrade the performance of standard **MTL** approaches [7]. In such settings, robustness to outliers and to variations in task difficulty or data quality is essential. However, robust techniques for **MTL** boosting have not been explored in existing research. Although previous work in **MTL** has introduced robust objectives and adaptive task weighting strategies [7, 15, 16], at least one such approach has not been successfully integrated into the **GB** framework.

To address this gap, we propose Robust-Multi-Task Gradient Boosting (**R-MTGB**), a novel multi-task boosting algorithm that can learn across tasks with varying degrees of relatedness. **R-MTGB** introduces a structured ensemble learning framework composed of three sequential blocks. In the first block, the model learns a shared representation that captures commonalities across all tasks. The second block distinguishes between outlier and non-outlier tasks by optimizing a regularized task-specific parameter, enabling adaptive weighting of task contributions. Finally, the third block performs fine-tuning by learning task-specific predictors, enabling the model to capture the nuances of individual tasks. This modular design allows **R-MTGB** to dynamically balance shared learning and task-specific adaptation,

improving generalization across heterogeneous task sets. As a result, the model is robust to noisy tasks, scalable to large datasets, and adaptable to a wide range of loss functions.

The key contributions of this study are as follows:

- We propose a novel **R-MTGB** framework based on **GB**, specifically designed to handle task-level noise and outliers in **MTL** problems.
- Our approach integrates outlier task detection directly into the Multi-Task Gradient Boosting (**MTGB**) process, allowing the model to identify and isolate anomalous tasks during training.
- The proposed model consists of three coordinated training blocks, enabling it to learn robust task representations and effectively distinguish between outlier and non-outlier tasks using task-specific parameters.
- Through controlled experiments on synthetic datasets, we empirically validate our hypothesis: the model successfully identifies outlier tasks while maintaining high performance on all tasks, demonstrating strong robustness in the presence of noisy training data.

The remainder of the paper is organized as follows. Section 2 presents the related studies on **MTL**, **GB**, and multi-task boosting frameworks. Section 3 outlines the methodology, including the mathematical foundation of the proposed approach. The experiments conducted and their detailed results are presented in Section 4. Finally, Section 5 provides a summary of the paper.

2 Related Work

This section reviews prior work relevant to our proposed approach. We begin by introducing the core ideas and categories of **MTL** in Subsection 2.1. In Subsection 2.2, we summarize the development of **GB** and its variants. Finally, in Subsection 2.3, we discuss prior attempts to apply boosting methods to multi-task problems and highlight the differences between these approaches and ours.

2.1 Multi-Task Learning

MTL is a **ML** approach in which multiple tasks are learned simultaneously, allowing shared knowledge across functions to improve overall performance [2]. The core assumption in **MTL** is that tasks within a given dataset are related [2, 17]. By leveraging transfer learning, **MTL** enables models to use information gained from one task to enhance learning and generalization on related tasks, leading to more robust and adaptable systems compared to training separate models for each task [1].

Several well-defined approaches to exploring **MTL** have been studied, including feature learning, low-rank parameterization, task clustering, task relationship modeling, and decomposition methods [1]. In feature learning, the objective is to discover a shared representation across multiple tasks by leveraging common features. This approach has been implemented in various **ML** models, including neural networks [2, 18] and deep neural networks [19, 20, 21, 22].

The Low-Rank methodology, on the other hand, is designed to capture the relatedness among tasks by assuming that the parameter matrix across tasks lies in a low-rank subspace [23]. This implies the existence of common latent factors shared among tasks. The objective is to minimize a joint loss function over the weight matrix, subject to a low-rank constraint (often via nuclear norm regularization or matrix factorization). Recent studies have applied this approach to develop **MTL** approaches in various areas, such as improving parameter-efficient training of multi-task models [24], identifying outliers [25], and reconstructing low-rank weight matrices [26].

Another approach in **MTL** involves grouping related tasks into clusters, as first proposed by [27], where it exploits the shared structure within each cluster to enhance learning. Later, a theoretical framework for **MTL** based on clustering tasks and assigning each cluster to one of a limited number of shared hypotheses was proposed [28]. This hard-assignment strategy facilitates learning from limited data while effectively controlling model complexity.

Another category in **MTL** focuses on approaches that encourage the model to treat the average of task-specific parameters as a central assumption, based on the idea that tasks are inherently similar [29, 30]. Other studies regularize the objective function by measuring pairwise task similarities [31] or controlling task relatedness [32].

Lastly, the decomposition approach involves breaking down model parameters into shared and task-specific components. This enables the model to learn common patterns across tasks while also capturing nuances unique to individual tasks. A study by [33] introduced an approach that simultaneously learns both shared and task-specific parameters directly from data by implementing a layered decomposition of the parameter matrix, with each layer representing a level in the task hierarchy. Another study decomposes the model parameters for each task into shared components and

task-specific deviations, applying a methodology to learn multiple related parameters tasks simultaneously [29]. This approach allows for better control over the shared information, with each task parameter vector represented as the sum of a common vector and a task-specific offset. In a related line of work, but using a different **ML** model, **MTGB** was introduced [12]. This approach explicitly incorporates both shared and task-specific components through a two-phase process. In the first phase, a common set of models is trained to capture patterns shared across all tasks. In the second phase, separate models are added for each task to learn the pseudo-residual information specific to that task.

2.2 Gradient Boosting

In the context of tabular datasets and supervised learning models, ensemble learning has demonstrated strong performance in solving a wide range of **ML** problems [10], including classification and regression [34, 35]. Ensemble models work by combining multiple weak learners to construct a more robust and accurate final model [36].

GB is among the most successful ensemble methods. It builds predictive models by sequentially adding weak regressors, typically Decision Tree Regressor (**DTR**), to correct the residuals of preceding models [37]. A faster variant of **GB** is XGBoost, which introduces regularization into the objective function and employs an improved branch-splitting method in **DTR**, resulting in faster training and enhanced accuracy [8]. Another notable advancement is LightGBM, which accelerates **GB** through novel sampling strategies and feature bundling methods, achieving high speed and performance [38]. CatBoost, further addresses prediction shifts in **GB** by introducing a permutation-based technique [39].

The strong performance of **GB** has led to the development of multi-class classification and multi-output regression models. These models extend **GB** and its variants to address such problems more efficiently by restructuring **GB** variants to support multi-output and multi-class problems within their loss functions and **DTRs**. Gradient-Boosted Decision Trees for Multiple Outputs represents the multi-output extension of XGBoost [40], while Condensed-Gradient Boosting is a multi-output version of **GB** that employs multi-output **DTRs** [41], which is also less complex than previous **GB** variants in terms of both time and space requirements. These developments highlight flexibility and potential of the **GB** framework for tackling more complex supervised learning problems involving multiple tasks.

2.3 Boosting Multi-Task Learning

The first study to develop a multi-task boosting approach was conducted by [11], where the authors leveraged **GB** to design a customize **MTL** framework. Their method maintains $T + 1$ boosted models composed of (**DTRs**): one global model to capture shared structure among all tasks and T task-specific models to account for individual task nuances. At each boosting iteration, the algorithm adds a new **DTR** to either the global or a task-specific model, depending on which yields the greatest reduction in the overall objective, determined via steepest descent. An ℓ_1 -norm regularization is imposed to promote sparsity in the learned functions. The overall objective is to iteratively optimize a shared loss function across tasks by selecting the direction (i.e., weak learner and task) that most improves the loss, as approximated through a first-order Taylor expansion. Another **MTL** framework built upon **GB** integrates **DTR** with deep neural network [42]. The boosting process is implemented in two distinct stages. In the first stage, a multi-task deep learning (MDL) network is trained across several related tasks to learn shared representations, effectively leveraging data-rich tasks to support those with limited data. In the second stage, the output from the final hidden layer of the MDL network is used as input features for training a **GB** model. Another study similar to the one proposed in [11] is the **MTGB** model, which differs in structure, framework, and optimization strategy [12]. **MTGB** builds on **GB** by explicitly separating the learning process into two components: common (shared) estimators and task-specific estimators. Hence, the optimization (derived by Newton-Raphson method) is performed in two stages: first, a shared loss function is minimized using the combined data from all tasks; then, task-specific loss functions are optimized separately for each task. An alternative approach that differs significantly from previous studies is the Boosted-**MTL** framework, which is based on a federated learning paradigm [43]. This framework operates in two sequential stages. First, in the *global learning* stage, multiple districts collaborate through a privacy-preserving federated **GB** scheme, known as FederBoost, to learn shared load patterns. Second, in the *local learning* stage, each district independently fine-tunes a local model to capture its district-specific load characteristics. The final model is constructed as the sum of the global and local **GB** models.

From a different perspective, rather than restructuring the **GB** framework, Task-wise Split-**GB** (TSGB) introduced a task-specific splitting mechanism [44]. This approach replaces the standard splitting criterion with one that separates samples based on task-specific performance, referred to as task gain. A split is performed only when the negative impact on other tasks does not exceed a predefined threshold. Later, an extension of TSGB was introduced to address the issue of imbalanced data by proposing two approaches: TSGB_β , which revises the task gain ratio to be more sensitive to the number of affected tasks rather than the number of instances; and TSGB_κ , which re-weights datasets using a softmax-based method to balance data distribution across tasks [45]. These adaptations enhance both overall

and task-specific prediction performance without compromising the accuracy for minority labels, as reported in a recent preprint [46].

Our proposed model falls into the first category of boosting **MTL** approaches. Unlike tree-based models or federated learning framework, our method redefines the ensemble structure to directly address challenges specific to **MTL**. While prior work in this category has largely focused on modeling shared and task-specific patterns, they have not addressed the presence of outlier or adversarial tasks, which can degrade overall model performance. To the best of our knowledge, no existing boosting or ensemble-based approach has systematically tackled this issue. Our model introduces an inner parameter optimization step that identifies and differentiates outlier or adversarial tasks during training. This not only improves robustness and pattern recognition but also enhances interpretability by allowing the clustering of tasks into inlier and outlier categories based on their behavior in the learning process.

3 Methodology

This section details the methodologies utilized throughout the study. It begins with the preliminaries and notation (Subsection 3.1), followed by introduction to **MTL** (Subsection 3.2). Next, an overview of **GB** framework (Subsection 3.3) is provided, leading to the presentation of the proposed **R-MTGB** extension and its underlying mathematical framework (Subsection 3.4).

3.1 Preliminaries and Notation

In this study, we define the input space as $\mathcal{X} \subseteq \mathbb{R}^d$, where each input $\mathbf{x} \in \mathcal{X}$ is a d -dimensional feature vector. The corresponding output space is $\mathcal{Y} \subseteq \mathbb{R}$, where each output $y \in \mathcal{Y}$ is a target scalar value.

The dataset is denoted by $\mathcal{D} = \{(\mathbf{x}_i, y_i)\}_{i=1}^N$, where each sample (\mathbf{x}_i, y_i) is drawn independently and identically distributed (i.i.d.) from $P(\mathcal{X}, \mathcal{Y})$, and N is the number of samples. This corresponds to a supervised learning setting, where the goal is to learn a mapping from inputs to outputs using labeled data.

Subsequently, to evaluate the performance of the training model, we define a loss function $\mathcal{L}(y, \hat{F})$, which measures the discrepancy between the true output y and the model output \hat{F} . The specific form of the loss function depends on the nature of the problem.

In this study, we use the cross-entropy loss function for classification,

$$\mathcal{L}(\mathbf{y}, \hat{\mathbf{F}}) = - \sum_{k=1}^K \mathbf{y}_k \ln(P_k), \quad (1)$$

where K is the number of distinct class labels, \mathbf{y} is a one-hot encoded class label vector with K different class labels, and P_k is the predicted probability of class k ,

$$P_k = \frac{\exp(\hat{F}_k)}{\sum_{k=1}^K \exp(\hat{F}_k)}. \quad (2)$$

For regression, we employ the squared error loss function,

$$\mathcal{L}(y, \hat{F}) = \frac{1}{2} (y - \hat{F})^2. \quad (3)$$

3.2 Multi-Task Learning

Considering a collection of T tasks, each task $t \in \{1, \dots, T\}$ is associated with its own input-output space, $\mathcal{X}^{(t)} \subseteq \mathbb{R}^{d^{(t)}}$ and $\mathcal{Y}^{(t)} \subseteq \mathbb{R}$, respectively. We assume a shared input space $\mathcal{X} = \mathcal{X}^{(1)} = \dots = \mathcal{X}^{(T)}$, with consistent feature dimensionality $d^{(t)} = d$ across all tasks. Similarly, the output space is shared among tasks, $\mathcal{Y} = \mathcal{Y}^{(1)} = \dots = \mathcal{Y}^{(T)}$. Each task t has its own dataset,

$$\mathcal{D}^{(t)} = \{(\mathbf{x}_{i,t}, y_{i,t})\}_{i=1}^{N^{(t)}}, \quad (4)$$

where $(\mathbf{x}_{i,t}, y_{i,t}) \sim P^{(t)}(\mathcal{X}^{(t)}, \mathcal{Y}^{(t)})$. While these tasks are generally assumed to be related, in practice, the collection may contain *outlier tasks* that deviate significantly from the common structure—due to noisy labels, data domain mismatch, or task-specific peculiarity. Such tasks can negatively impact the quality of the shared representation and degrade overall performance if treated uniformly within the learning process.

The goal of **MTL** is to simultaneously learn a collection of task-specific functions,

$$\{F^{(t)} : \mathcal{X}^{(t)} \rightarrow \mathcal{Y}^{(t)}\}_{t=1}^T,$$

that collectively minimize the total loss across all tasks,

$$F(\mathbf{x}) = \operatorname{argmin}_{\{\hat{F}^{(t)}\}_{t=1}^T} \sum_{t=1}^T \sum_{i=1}^{N^{(t)}} \left[\mathcal{L}(y_{i,t}, \hat{F}^{(t)}(\mathbf{x}_{i,t})) \right]. \quad (5)$$

To facilitate parameter sharing across tasks, **MTL** models can alternatively express each task-specific function $F^{(t)}$ as the *sum* of a shared component and a task-specific component,

$$F^{(t)}(\mathbf{x}) = \phi(\mathbf{x}) + \psi^{(t)}(\mathbf{x}), \quad (6)$$

where $\phi : \mathcal{X} \rightarrow \mathcal{Y}$ denotes a *shared function* capturing common structure across tasks, and $\psi^{(t)} : \mathcal{X}^{(t)} \rightarrow \mathcal{Y}^{(t)}$ is a *task-specific function* modeling individual task characteristics. This additive formulation enables the model to learn a global inductive bias via ϕ , while still allowing per-task flexibility through $\psi^{(t)}$. However, the presence of outlier tasks—which do not align well with the dominant task structure—can mislead the learning of the shared representation ϕ , resulting in degraded performance across the entire task set.

3.3 Gradient Boosting

The primary objective of **GB** model, as introduced by [37], is to iteratively minimize a given loss $\mathcal{L}(y, \hat{F}(\mathbf{x}))$, by finding a function that maps the input features \mathbf{x} to the predicted output \hat{F} ,

$$F(\mathbf{x}) = \operatorname{argmin}_{\hat{F}(\mathbf{x})} \sum_{i=1}^N \left[\mathcal{L}(y_i, \hat{F}(\mathbf{x}_i)) \right]. \quad (7)$$

This optimization is performed forward stage-wise by sequentially adding weak learners $h_m(\mathbf{x})$ (**DTR**) and incorporating the ensemble parameter γ at each boosting epoch m to the model,

$$\hat{F}_M(\mathbf{x}) = \sum_{m=0}^M \gamma_m h_m(\mathbf{x}), \quad (8)$$

where it is initialized with a constant value that minimizes the loss,

$$\hat{F}_0(\mathbf{x}) = \operatorname{argmin}_{\gamma} \sum_{i=1}^N \mathcal{L}(y_i, \gamma). \quad (9)$$

Hence, Eq. (7) can be expressed as a stage-wise greedy process,

$$(\gamma_m, h_m) = \operatorname{argmin}_{\{\gamma_m, h_m\}} \sum_{i=1}^N \mathcal{L}(y_i, \hat{F}_{m-1}(\mathbf{x}_i) + \gamma_m h_m(\mathbf{x}_i)). \quad (10)$$

At each iteration m , instead of directly optimizing Eq. (10), **GB** utilizes the negative gradient of the loss function (pseudo-residuals) with respect to the prediction of the current model to guide the learning of the next weak learner,

$$r_{i,m} = - \left[\frac{\partial \mathcal{L}(y_i, \hat{F}(\mathbf{x}_i))}{\partial \hat{F}(\mathbf{x}_i)} \right]_{F=\hat{F}_{m-1}(\mathbf{x}_i)}, \quad (11)$$

for each sample i in the dataset. A new weak learner $h_m(\mathbf{x})$ is then fitted to these residuals by minimizing the squared error (regardless of the loss function the ensemble is trying to optimize),

$$h_m(\mathbf{x}) = \operatorname{argmin}_{\{h \in \mathcal{H}\}} \sum_{i=1}^N (r_{i,m} - h_m(\mathbf{x}_i))^2, \quad (12)$$

where \mathcal{H} denotes the hypothesis space of weak learners (DTR). Once the weak learner $h_m(\mathbf{x})$ is determined, the optimal parameter γ_m is obtained by solving the line search problem,

$$\gamma_m = \operatorname{argmin}_{\gamma_m} \sum_{i=1}^N \mathcal{L} \left(y_i, \hat{F}_{m-1}(\mathbf{x}_i) + \gamma_m h_m(\mathbf{x}_i) \right). \quad (13)$$

Note that for squared error loss, $\gamma_m = 1$ is typically optimal. As a result, the explicit line search (Eq. (13)) is frequently omitted in practice, which simplifies the update process.

After M boosting iterations, the final predictive model is built as an additive ensemble of weak learners,

$$F(\mathbf{x}) = \hat{F}_M(\mathbf{x}) = \hat{F}_0(\mathbf{x}) + \eta \sum_{m=1}^M \gamma_m h_m(\mathbf{x}), \quad (14)$$

where $\eta \in (0, 1]$ is a learning rate, that is used to regularize the gradient descent steps in the learning process.

GB has consistently shown strong empirical performance across a diverse set of **ML** tasks, including regression [47, 48], binary and multiclass classification [49, 50], ranking [51], missing value estimation [52], and multi-task problems [11, 43, 12]. Its flexibility in accommodating different loss functions makes it well-suited for both standard and specialized applications [53, 9].

3.4 Robust Multi-Task Gradient Boosting

To address challenges in multi-task settings, such as task heterogeneity and outlier influence, we propose a three-stage **GB** framework called **R-MTGB**, which integrates robustness and shared representation learning within the **MTGB** paradigm. The training process of the proposed **R-MTGB** model is divided into three sequential blocks, each designed to address a specific aspect of **MTL** challenge:

- **Block 1** Focuses on shared representation learning by leveraging all tasks jointly to identify a common feature space that captures task-invariant patterns.
- **Block 2** Introduces robustness to task outliers by distinguishing between inlier and outlier tasks through a regularization mechanism that allocates extreme weights to outlier tasks—amplifying reliable tasks while suppressing the influence of outlier tasks—thereby enabling the model to focus on the most informative task signals.
- **Block 3** Performs task-specific refinement, where individual models are fine-tuned for each task based on the previously learned shared and robust representations.

Each block builds upon the outputs of the previous blocks, progressively refining the model to improve performance across both related and unrelated tasks. Formally, the total number of boosting iterations M is partitioned into three phases:

$$M = M_1 + M_2 + M_3,$$

where M_1 , M_2 , and M_3 correspond to the iterations assigned to Block 1, Block 2, and Block 3, respectively.

The overall proposed ensemble prediction function for a given input \mathbf{x} is

$$F_t(\mathbf{x}) = \hat{F}^{(\text{shared})}(\mathbf{x}) + (1 - \sigma(\theta_t)) \hat{F}^{(\text{non-outlier})}(\mathbf{x}) + \sigma(\theta_t) \hat{F}^{(\text{outlier})}(\mathbf{x}) + \hat{F}_t^{(\text{task})}(\mathbf{x}), \quad (15)$$

where,

- \hat{F}^{shared} is the shared-model that captures global shared structures across all tasks.
- $\hat{F}^{\text{non-outlier}}$ models patterns characteristic of non-outlier tasks.
- \hat{F}^{outlier} captures patterns specific to outlier tasks.
- \hat{F}^{task} represents the task-specific fine-tuned model for unique task-level information.
- $\sigma(\theta_t) = \frac{1}{1 + \exp(-\theta_t)}$ is the sigmoid function applied element-wise to the θ_t , controlling the interpolation between the outlier and non-outlier components for each task.

Although the ensemble prediction function (Eq. (15)) contains four components, they are learned through three training blocks. Specifically, Block 2 jointly models both the outlier and non-outlier terms via a unified regularization mechanism that allocates task-specific weights. This shared optimization process gives rise to two separate components in the second block.

Each predictor $h_m^{(\cdot)}$ is trained by minimizing a stage-specific loss over the data instances associated with that stage. Where $(\cdot) \in \{M_1, M_2, M_3\}$, and let $M_{(\cdot)}$ denote the number of boosting iterations allocated to that component. Then, the general training objective for all blocks is,

$$\begin{aligned} \min_{\{h_m^{(\cdot)}\}_{m=1}^{M_{(\cdot)}}} \sum_{t=1}^T \sum_{i=1}^{N_t} \left[\sum_{m=1}^{M_1} \mathcal{L} \left(h_m^{(\text{shared})}(\mathbf{x}_{i,t}), r_{i,m,t}^{(\text{shared})} \right) \right. \\ + \sum_{m=M_1+1}^{M_1+M_2} \left(\mathcal{L} \left(h_m^{(\text{outlier})}(\mathbf{x}_{i,t}), r_{i,m,t}^{(\text{outlier})} \right) + \right. \\ \left. \mathcal{L} \left(h_m^{(\text{non-outlier})}(\mathbf{x}_{i,t}), r_{i,m,t}^{(\text{non-outlier})} \right) \right) \\ \left. + \sum_{m=M_1+M_2+1}^M \mathcal{L} \left(h_m^{(\text{task})}(\mathbf{x}_{i,t}), r_{i,m,t}^{(\text{task})} \right) \right] \end{aligned} \quad (16)$$

where $\mathbf{x}_{i,t}$ is the input for instance i in task t , $r_{i,m,t}^{(\cdot),(t)}$ is the corresponding residual at iteration m for component (\cdot) , and $h_m^{(\cdot)}$ refers to the m -th DTR, implemented as a single-level tree predictor. In the case of multi-class classification $h_m^{(\cdot)}$ is a multi-output tree, as employed in [41], where class probabilities are obtained by applying the soft-max activation function to the aggregated outputs across all iterations.

Note: The pseudo-residuals $r_{i,m,t}^{(\cdot)}$ are recalculated at every boosting iteration m within their respective block ranges M_1 , M_2 , and M_3 . This ensures that each new weak learner fits the current negative gradient of the loss with respect to the ensemble prediction, enabling iterative refinement of the model components throughout training.

Block 1: shared-Learning via Data Pooling

In the first stage, a common base of predictive models is learned by training M_1 shared-level predictors, $h_m^{(\text{shared})}(\mathbf{x}_i, r_{i,m,t}^{\text{shared}})$ using data from all tasks,

$$\mathcal{D}_{\text{pool}} = \bigcup_{t=1}^T \mathcal{D}^{(t)}, \quad (17)$$

and pseudo-residuals,

$$\begin{aligned} r_{i,m,t}^{(\text{shared})} &= -\frac{\partial \mathcal{L}(y_{i,t}, F(\mathbf{x}_{i,t}))}{\partial \hat{F}^{(\text{shared})}(\mathbf{x}_{i,t})} \\ &= -\frac{\partial \mathcal{L}(y_{i,t}, F(\mathbf{x}_{i,t}))}{\partial F(\mathbf{x}_{i,t})} \cdot \frac{\partial F(\mathbf{x}_{i,t})}{\partial \hat{F}^{(\text{shared})}(\mathbf{x}_{i,t})} \\ &= -\left[\frac{\partial \mathcal{L}(y_{i,t}, F(\mathbf{x}_{i,t}))}{\partial F(\mathbf{x}_{i,t})} \right]_{F=F_{m-1}^{(\text{shared})}(\mathbf{x}_i)}, \end{aligned} \quad (18)$$

and updates the ensemble as defined in Eq. (15).

Block 2: Outlier-Aware Task Partitioning

To mitigate the impact of task outliers, the second block adopts a two-component structure over the pooled data $\mathcal{D}_{\text{pool}}$: (1) one component targets outlier tasks, (2) while the other focuses on non-outlier tasks.

The outlier component is obtained by fitting $h_m^{(\text{outlier})}(\mathbf{x}_i, r_{i,m,t}^{(\text{outlier})})$, to the negative gradient of the loss with respect to $F^{(\text{outlier})}$,

$$\begin{aligned} r_{i,m,t}^{(\text{outlier})} &= -\frac{\partial \mathcal{L}(y_{i,t}, F(\mathbf{x}_{i,t}))}{\partial \hat{F}^{(\text{outlier})}(\mathbf{x}_{i,t})} \\ &= -\frac{\partial \mathcal{L}(y_{i,t}, F(\mathbf{x}_{i,t}))}{\partial F(\mathbf{x}_{i,t})} \cdot \frac{\partial F(\mathbf{x}_{i,t})}{\partial \hat{F}^{(\text{outlier})}(\mathbf{x}_{i,t})}, \end{aligned} \quad (19)$$

which yields,

$$r_{i,m,t}^{(\text{outlier})} = - \left[\frac{\partial \mathcal{L}(y_{i,t}, F(\mathbf{x}_{i,t}))}{\partial F(\mathbf{x}_{i,t})} \right]_{F=F_{m-1}^{(\text{outlier})}(\mathbf{x}_i)} \cdot \sigma(\theta_t). \quad (20)$$

In a similar manner, we obtain the non-outlier component by fitting $h_m^{\text{non-outlier}}(\mathbf{x}_i, r_{i,m}^{\text{non-outlier}})$, to the negative gradient of the loss with respect to $F^{\text{non-outlier}}$,

$$\begin{aligned} r_{i,m,t}^{(\text{non-outlier})} &= - \frac{\partial \mathcal{L}(y_{i,t}, F(\mathbf{x}_{i,t}))}{\partial \hat{F}^{(\text{non-outlier})}(\mathbf{x}_{i,t})} \\ &= - \frac{\partial \mathcal{L}(y_{i,t}, F(\mathbf{x}_{i,t}))}{\partial F(\mathbf{x}_{i,t})} \cdot \frac{\partial F(\mathbf{x}_{i,t})}{\partial \hat{F}^{(\text{non-outlier})}(\mathbf{x}_{i,t})}, \end{aligned} \quad (21)$$

which gives,

$$r_{i,m,t}^{(\text{non-outlier})} = - \left[\frac{\partial \mathcal{L}(y_{i,t}, F(\mathbf{x}_{i,t}))}{\partial F(\mathbf{x}_{i,t})} \right]_{F=F_{m-1}^{(\text{non-outlier})}(\mathbf{x}_i)} \cdot (1 - \sigma(\theta_t)). \quad (22)$$

Block 2 leverages the parameter θ_t , which dynamically adjusts the influence of each task t through a sigmoid-based weighting mechanism. Rather than explicitly labeling tasks as outliers or inliers, the model is encouraged to learn a soft partitioning, where the sigmoid activations of θ_t tend toward—but do not always reach—extreme values close to 0 or 1. This soft activation enables flexible modulation of the contribution of each task to the outlier and non-outlier components. By doing so, the model can reduce the influence of anomalous tasks while emphasizing signals from more consistent ones. As training progresses, gradients of the loss function \mathcal{L} with respect to parameter vector θ guide this modulation, allowing the optimization process to adaptively infer and separate outlier behavior in a data-driven manner,

$$\begin{aligned} -\frac{\partial \mathcal{L}}{\partial \theta} &= -\frac{\partial \mathcal{L}}{\partial F} \cdot \frac{\partial F}{\partial \theta} \\ &= - \sum_{t=1}^T \sum_{i=1}^{N^{(t)}} \frac{\partial \mathcal{L}(y_{i,t}, F(\mathbf{x}_{i,t}))}{\partial F(\mathbf{x}_{i,t})} \cdot \frac{\partial F(\mathbf{x}_{i,t})}{\partial \theta}, \end{aligned} \quad (23)$$

where,

$$\begin{aligned} -\frac{\partial F}{\partial \theta} &= -\sigma(\theta)(1 - \sigma(\theta)) \hat{F}^{(\text{non-outlier})}(\mathbf{x}) \\ &\quad + \sigma(\theta)(1 - \sigma(\theta)) \hat{F}^{(\text{outlier})}(\mathbf{x}). \end{aligned} \quad (24)$$

Block 3: Task-Specific Fine-Tuning

The final block shifts focus to per-task specialization, where each task-fine-tuning individual task models using exclusively their local data. This block operates as a standard Single Task (ST)-GB, initialized with the accumulated models from previous blocks.

Each task independently fits $h_m^{(\text{task})}(\mathbf{x}_i, r_{i,m}^{(\text{task})})$, to the corresponding pseudo-residuals,

$$\begin{aligned} r_{i,m,t}^{(\text{task})} &= - \frac{\partial \mathcal{L}(y_{i,t}, F(\mathbf{x}_{i,t}))}{\partial \hat{F}^{(\text{task})}(\mathbf{x}_{i,t})} \\ &= - \frac{\partial \mathcal{L}(y_{i,t}, F(\mathbf{x}_{i,t}))}{\partial F(\mathbf{x}_{i,t})} \cdot \frac{\partial F(\mathbf{x}_{i,t})}{\partial \hat{F}^{(\text{task})}(\mathbf{x}_{i,t})} \\ &= - \left[\frac{\partial \mathcal{L}(y_{i,t}, F(\mathbf{x}_{i,t}))}{\partial F(\mathbf{x}_{i,t})} \right]_{F=F_{m-1}^{(\text{task})}(\mathbf{x}_i)}. \end{aligned} \quad (25)$$

This stage allows each task to capture unique patterns not shared by previous blocks.

Finally, considering the choice of the loss function for each problem type, the residuals and gradients are computed differently for classification and regression tasks. For classification, using the cross-entropy loss (Eq. (1)), the residuals are defined as the difference between the true labels and predicted probabilities (Eq. (2)),

$$r_{i,k} = y_{i,k} - P_{i,k}(\mathbf{x}_i), \quad (26)$$

For regression with true outputs y_i and the squared error loss defined in Eq. (3), the residual is given by the difference between the true and predicted outputs,

$$r_i = y_i - \hat{F}(\mathbf{x}_i). \quad (27)$$

Consequently, the negative gradient of the loss with respect to the parameter $\theta^{(t)}$ (Eq. (23)) is computed as,

$$\begin{aligned} -\frac{\partial \mathcal{L}}{\partial \theta^{(t)}} = & -r_{i,t} \cdot \sigma(\theta^{(t)}) \cdot (1 - \sigma(\theta^{(t)})) \\ & \cdot \left[\hat{F}^{(\text{outlier}), (t)}(\mathbf{x}_{i,t}) - \hat{F}^{(\text{non-outlier}), (t)}(\mathbf{x}_{i,t}) \right] \end{aligned} \quad (28)$$

The training procedure of the proposed **R-MTGB** is summarized in algorithm 1.

Algorithm 1: Robust-Multi-Task Gradient Boosting (**R-MTGB**) Training Procedure

Input : $\{\mathcal{D}^{(t)}\}_{t=1}^T, \mathcal{L}, M = M_1 + M_2 + M_3, \eta \in (0, 1], \theta \sim \mathcal{N}(\mu, \sigma^2)$

Output: $F(\mathbf{x})$

Initialize: $\hat{F}_0^{\text{shared}} = \hat{F}_0^{\text{outlier}} = \hat{F}_0^{\text{non-outlier}} = \hat{F}_0^{\text{task}} = 0, \mathcal{D}_{\text{pool}} = \bigcup_{t=1}^T \mathcal{D}^{(t)}$

Block 1: shared-Learning:

for $m = 1$ **to** M_1 **do**

$$\begin{cases} \forall t, i : r_{i,m}^{(\text{shared}), (t)} \leftarrow \text{Eq. (18)}; \\ h_m^{(\text{shared})} \leftarrow \text{fit}(\mathcal{D}_{\text{pool}}, r_m^{(\text{shared})}); \\ \hat{F}_m^{(\text{shared})} \leftarrow \hat{F}_{m-1}^{(\text{shared})} + \eta h_m^{(\text{shared})} \end{cases}$$

Block 2: Outlier Partitioning:

for $m = (M_1 + 1)$ **to** $(M_1 + M_2)$ **do**

$$\begin{cases} \forall t, i : r_{i,m}^{(\text{outlier}), (t)} \leftarrow \text{Eq. (20)}, r_{i,m}^{(\text{non-outlier}), (t)} \leftarrow \text{Eq. (22)}; \\ h_m^{(\text{outlier})} \leftarrow \text{fit}(\mathcal{D}_{\text{pool}}, r_m^{(\text{outlier})}), \hat{F}_m^{(\text{outlier})} \leftarrow \hat{F}_{m-1}^{(\text{outlier})} + \eta h_m^{(\text{outlier})}; \\ h_m^{(\text{non-outlier})} \leftarrow \text{fit}(\mathcal{D}_{\text{pool}}, r_m^{(\text{non-outlier})}), \hat{F}_m^{(\text{non-outlier})} \leftarrow \hat{F}_{m-1}^{(\text{non-outlier})} + \eta h_m^{(\text{non-outlier})}; \\ \forall t : \theta_m^{(t)} \leftarrow \theta_{m-1}^{(t)} - \eta \frac{\partial \mathcal{L}}{\partial \theta_{m-1}^{(t)}} \text{ using Eq. (24)}; \end{cases}$$

Block 3: Task-Specific Fine-Tuning:

for $m = (M_1 + M_2 + 1)$ **to** M **do**

$$\begin{cases} \text{for } t = 1 \text{ to } T \text{ do} \\ \quad \forall i : r_{i,m}^{(\text{task}), (t)} \leftarrow \text{Eq. (25)}; \\ \quad h_m^{(\text{task}), (t)} \leftarrow \text{fit}(\mathcal{D}^{(t)}, r_m^{(\text{task}), (t)}); \\ \quad \hat{F}_m^{(\text{task}), (t)} \leftarrow \hat{F}_{m-1}^{(\text{task}), (t)} + \eta h_m^{(\text{task}), (t)} \end{cases}$$

return $\hat{F}^{(\text{shared}), (t)}(\mathbf{x}) + (1 - \sigma(\theta^{(t)}))\hat{F}^{(\text{non-outlier}), (t)}(\mathbf{x}) + \sigma(\theta^{(t)})\hat{F}^{(\text{outlier}), (t)}(\mathbf{x}) + \hat{F}^{(\text{task}), (t)}(\mathbf{x})$

4 Experiments and Results

This section outlines the experimental setup and methodology used to evaluate the performance of the proposed model. The experiments were designed to assess the effectiveness of the proposed approach compared to state-of-the-art models and analyze its behavior under varying conditions. Subsection 4.1 details the experimental setup and studied models, followed by Subsection 4.2 which describes the datasets used in the experiments. Subsection 4.3 describes the synthetic experiments conducted to validate the robustness of the proposed model and to address the hypothesis of the study. Finally, the results of real-world datasets and their interpretations are presented in Subsection 4.4.

4.1 Setup

To conduct the experiments, a combination of physical computing resources and developed code was utilized to support both the training and evaluation of the proposed and state-of-the-art models. The model was developed using Python (version 3.9), and scikit-learn (version 1.6)². For transparency and reproducibility, the complete

²github.com/scikit-learn

codebase, with the preprocessed dataset, has been made publicly accessible through the associated GitHub repository ³.

To evaluate the proposed **R-MTGB** model, we conducted experiments alongside state-of-the-art models. These include: (1) conventional multi task model (**MTGB**) [12]; (2) **ST-GB**, a standard **GB** model trained independently for each task; (3) a pooled approach where a standard **GB** model is trained on data from all tasks combined (Data Pooling (**DP-GB**)); and (4) a Task as Feature (**TaF-GB**), which is another pooling approach using augmented input data where a one-hot encoding of the task identifiers is concatenated to the original features. It should be mentioned that the core implementation of **GB**, **TaF-GB**, and **DP-GB** is based on the standard **GB** framework proposed by [37]. The models were trained and evaluated by randomly splitting the data into training and testing subsets using an 80:20 ratio. This involved partitioning the arrays or matrices into random training (80%) and testing (20%) sets to ensure unbiased assessment of model performance. To ensure the reliability and robustness of the results, this process was repeated across 100 independent experimental batches.

To ensure consistent reporting and facilitate fair comparisons of model performance, hyperparameter optimization was performed using a within-training GridSearchCV method with a 5-fold cross-validation strategy. This procedure was applied to both the synthetic experiments (see Subsection 4.3) and the real-world case study (see Subsection 4.4). GridSearchCV exhaustively evaluates combinations of specified hyperparameters to identify the optimal configuration based on predefined evaluation metrics (Negative Root Mean Squared Error (**RMSE**) for regression models and accuracy for classification models in this study) [54]. Notably, all compared methods can be viewed as particular instances of the proposed **R-MTGB** framework, differentiated by the use of different blocks. This generalization allows **R-MTGB** to flexibly encompass a wide range of model configurations under a unified framework. The ranges of hyperparameter values explored for each method are summarized in Table 1. Hyperparameters not listed in the table were set to their default values as defined in the `scikit-learn` library. Additionally, decision stumps were used as the base learner for all the studied models.

Table 1: Hyperparameter grid reporting number of estimators for each model.

Model	No. of Estimators		
	1st Block	2nd Block	3rd Block
R-MTGB	[0, 20, 30, 50]	[20, 30, 50]	[0, 20, 30, 50, 100]
MTGB	[20, 30, 50]	–	[0, 20, 30, 50, 100]
ST-GB	–	–	[20, 30, 50, 100]
DP-GB	[20, 30, 50, 100]	–	–
TaF-GB	[20, 30, 50, 100]	–	–

4.2 Datasets

Table 2 provides a summary of the datasets used in this study, including the number of instances, features, and tasks associated with each dataset. The datasets are categorized into two main classification and regression types. The classification datasets include:

- **Avila** [55]: Recently published *Avila* dataset comprises 800 images extracted from the *Avila Bible*, a massive Latin manuscript of the complete *Bible* produced in the 12th century, likely between Italy and Spain. The primary objective of this imbalanced classification task is to attribute each image to one of the twelve identified copyists involved in its creation. In this study, we define the multi-task problem by treating the unique row numbers as representative patterns associated with individual scribes.
- **Adult** [56]: The *Adult* dataset is widely used in various studies as a benchmark for **MTL** [57, 58]. Its primary objective is to predict whether an individual earns more than 50K per year based on demographic data. The tasks are defined by dividing the population into gender and race categories, resulting in two datasets.
- **Bank Marketing** [59]: This open-source dataset originates from direct marketing campaigns conducted by a Portuguese banking institution. The objective is to predict whether a client will subscribe to a term deposit. In this study, tasks are defined based on the occupational categories of clients of the bank.

³github.com/GAA-UAM/R-MTGB

- **Landmine** [60]: *Landmine* dataset is designed for evaluating **MTL** algorithms in the context of landmine detection. The main task is to identify whether landmines are present in an image based on sensor data. The dataset is split into 29 tasks, each corresponding to a specific landmine. The *Landmine* dataset is a widely used resource for evaluating **MTL** algorithms in recent studies [61, 12].

The regression datasets include:

- **Abalone** [62]: The objective of this dataset is to predict the age of abalone specimens based on their physical measurements and features. The problem is structured as a multi-task challenge, involving three distinct tasks: predicting the age of male, female, and infant abalones. This dataset has recently been employed in various studies as a benchmark for **MTL** models [63, 64].
- **Computer** [65]: This is a survey dataset collected from 190 individuals, where participants were asked to rate the likelihood of purchasing a computer with various configurations, such as CPU, RAM, price, and other specifications. This dataset has been used in several studies as training data for multi-task models [66, 67, 12].
- **Parkinsons** [68]: This dataset consists of biomedical voice measurements from 42 individuals with early-stage disease of parkinson, collected over six months using a telemonitoring system installed in the homes of patients. The tasks involve predicting the Unified Parkinson’s Disease Rating Scale (UPDRS) scores, which assess the severity of motor symptoms. This dataset has been widely used to evaluate the performance of **ML** models in various studies [69, 70].
- **SARCOS** [71]: The *SARCOS* dataset is a widely used benchmark for regression tasks in robotic manipulation. The objective is to predict the torque required at each joint of a robotic arm based on 21-dimensional input features, which include joint angles and velocities measured at each of the seven joints (tasks). This dataset has been employed in numerous studies as a standard benchmark for **MTL** models [72, 73, 74].
- **School** [75]: The *school* dataset consists of evaluations from 139 secondary schools conducted over the years 1985, 1986, and 1987. It represents a random 50% sample, including data from 15, 362 students. This dataset is widely used in literature as one of the multi-task datasets [29, 11].

Table 2: Dataset description.

Name	Instances	Attributes	Tasks	Labels
Classification				
Avila	20, 867	10	48	12
Adult	48, 842	14	7	2
Bank Marketing	45, 211	16	12	2
Landmine	14, 820	9	29	2
Regression				
Abalone	4, 177	8	3	-
Computer	3, 800	13	190	-
Parkinsons	5, 875	19	42	-
SARCOS	342, 531	21	7	-
School	15, 362	10	139	-

4.3 Synthetic Experiments

We conducted a series of experiments using synthetic data to validate the robustness of the proposed **R-MTGB** model and to test our hypothesis prior to evaluation on real-world datasets. These synthetic datasets were generated using a combination of common ($\phi(\mathbf{x})$) and task-specific ($\psi^{(t)}(\mathbf{x})$) functions based on Random Fourier Features [76]. Considering a multi-task dataset $\mathcal{D}^{(t)}$ as defined in Eq. (4) and,

$$\mathbf{x}_{i,t} \sim \mathcal{U}([-1, 1]^d), \quad \forall i = 1, \dots, N^{(t)},$$

for a given input $\mathbf{x} \in \mathbb{R}^d$, the function output is generated with

$$F(\mathbf{x}) = \sum_{i=1}^N \theta_i \sqrt{\frac{2\alpha}{D}} \cos \left(\mathbf{w}_i^\top \frac{\mathbf{x}}{d_x} + b_i \right), \quad (29)$$

where,

- $\mathbf{w}_i \sim \mathcal{N}(\mathbf{0}, \mathbf{I})$ represents random frequencies.
- $b_i \sim \mathcal{U}(0, 2\pi)$ shifts random phase.
- $\theta_i \sim \mathcal{N}(0, 1)$ weights the random feature.
- $d_x = \text{length_scale} \cdot d$ is a scaling factor for smoothness.
- D is the number of random features.

By using this generation process, the latent functions are approximately sampled from a Gaussian process (GP) prior, as the Random Fourier Feature representation provides an explicit approximation of functions drawn from a stationary GP.

For a set of T tasks, a *shared* function generator can be defined $F^{(\text{shared})}(\mathbf{x})$ as a combination of a common function and a task-specific function,

$$F^{(\text{shared})}(\mathbf{x}) = \sum_{t=1}^T w \cdot \phi(\mathbf{x}^{(t)}) + (1 - w) \cdot \psi^{(t)}(\mathbf{x}^{(t)}), \quad (30)$$

where,

- ϕ is a shared function across all common tasks,
- $\psi^{(t)}$ is a task-specific function for task t ,
- and $w = 0.9$ is the combination weight.

Outlier tasks, on the other hand, are generated by replacing the shared function ϕ with a different function ϕ^{out} that is independently sampled,

$$F^{(\text{out})}(\mathbf{x}) = \sum_{t=1}^{\mathcal{T}_{\text{out}}} w \cdot \phi^{\text{out},(t)}(\mathbf{x}) + (1 - w) \cdot \psi^{(t)}(\mathbf{x}^{(t)}), \quad (31)$$

where, $|\mathcal{T}_{\text{out}}| = T_{\text{out}}$. Finally, the output for each task is generated by using the function output directly for regression

$$y_{i,t} = F^{(t)}(\mathbf{x}_{i,t}), \quad (32)$$

and binarizing it using the sign function for classification,

$$y_{i,t} = \text{sign}(F^{(t)}(\mathbf{x}_{i,t})), \quad (33)$$

where to maintain class balance across classification tasks, each class contains at least 10% of the samples.

An example of a generated toy dataset with one input and one output dimension, comprising seven common tasks and one outlier task, is illustrated in Figure 1. The figure shows that the common tasks (tasks one to seven) cluster together and form a coherent band, indicating that they share an underlying functional structure ($g^{(\text{shared}), (t)}(\mathbf{x})^{(t)}$). In contrast, task eight is distinguishable as an outlier. Its data points diverge significantly from the smooth patterns observed in the other tasks, exhibiting a noisier and less structured behavior. This distinction arises because task eight was generated using $g^{(\text{out}), (t)}(\mathbf{x})$.

We generated 100 random batches of a synthetic toy dataset, with each task comprising 300 training and 1,000 testing instances with five input features. Each batch included 10 tasks in total, two of which (last two tasks) were designated as outliers. For each batch of experiments, the models were trained using a fixed learning rate of one and a decision stump as the base estimator. The number of estimators was tuned via GridSearchCV using the hyperparameter grid defined in Table 1. The best set of hyperparameters found was then used for training and testing. The performance of the evaluated models was measured using recall and accuracy for classification problems (Table 3), and Root Mean Squared Error (RMSE) and Mean Absolute Error (MAE) for regression problems (Table 4). For each method, results were first averaged across all tasks and instances, followed by computing the overall average and standard deviation over multiple runs per batch. The best-performing values per dataset are indicated in boldface.

Table 3 shows that the proposed **R-MTGB** model achieves the highest test recall and accuracy among all evaluated methods, indicating strong generalization to unseen data. Although **ST-GB** obtained the best performance on the training set, its lower scores on the test set suggest potential overfitting.

Regarding the regression datasets, Table 4 shows that the proposed **R-MTGB** model achieved the lowest **MAE** and **RMSE** on the test set, indicating the most accurate and robust regression performance on unseen data. As in the classification task, **ST-GB** achieved slightly better performance on the training set, but exhibited higher test errors

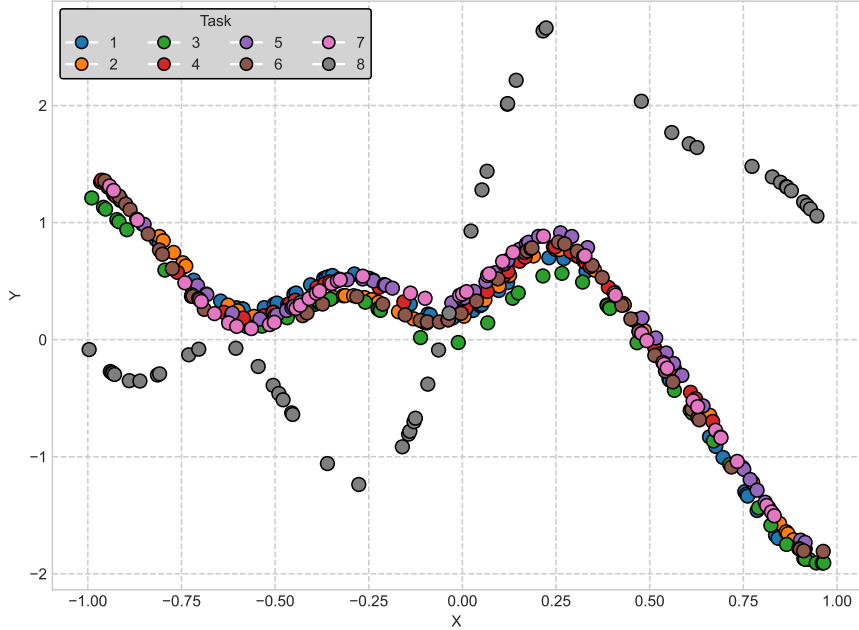


Figure 1: A visualization of the distribution of generated data points.

Table 3: Average Recall and Accuracy scores, along with their standard deviations, computed by first averaging across all instances and tasks, then averaging over multiple runs for each evaluated model on both training and testing synthetic datasets. Best-performing values per dataset are indicated in **boldface**.

	Recall		Accuracy	
	Train	Test	Train	Test
MTGB	0.895 ± 0.080	0.824 ± 0.108	0.905 ± 0.039	0.839 ± 0.042
DP-GB	0.773 ± 0.173	0.755 ± 0.182	0.794 ± 0.047	0.778 ± 0.049
R-MTGB	0.882 ± 0.090	0.829 ± 0.108	0.893 ± 0.046	0.843 ± 0.042
ST-GB	0.901 ± 0.083	0.819 ± 0.114	0.911 ± 0.039	0.834 ± 0.043
TaF-GB	0.801 ± 0.144	0.782 ± 0.154	0.816 ± 0.042	0.800 ± 0.045

compared to **R-MTGB**, again suggesting potential overfitting. In contrast, the performance of **R-MTGB** remained consistent across training and testing for both problems, highlighting its ability to generalize effectively to unseen data. The reason why the training evaluation results do not approach the extremes is that the training algorithm optimized the number of estimators (decision stumps) to minimize overfitting. This careful selection along with the use of decision stumps prevents the model from producing extreme outcomes during training analysis.

To further evaluate the performance of the task-wise models across the generated synthetic multi-task datasets, Figure 2 presents the average performance and standard deviation of each model on the unseen portion of the synthetic dataset, computed per task over 100 runs for each batch of experiments. Results are shown separately for classification tasks using accuracy (left subplot) and regression tasks using RMSE (right subplot). Each model is depicted in a distinct color, with vertical lines around the means representing the standard deviation. From Figure 2, it is evident that the proposed **R-MTGB** model outperforms both **MTGB** and **ST-GB** in all regression and most classification tasks. For classification (Figure 2, left subplot), the proposed **R-MTGB** model achieves the highest mean accuracy in the common tasks. For the outlier tasks, the studied models demonstrate comparable performance. **R-MTGB** model surpasses the **MTGB** model, whereas the **ST-GB** model performs negligibly better than **R-MTGB** model. Moreover, for regression tasks (Figure 2, right subplot), **R-MTGB** outperforms all models, including on outlier tasks, demonstrating robustness and effective utilization of information from common tasks to maintain strong performance across all tasks. Importantly, the absence of a weighting mechanism to identify outliers, causes the conventional **MTGB** approach to underperform in outlier tasks across both problem settings, compared to **ST-GB** model.

To assess the ability of the proposed model to detect and identify the two determined outlier tasks in the synthetic dataset, the mean and standard deviation of the learned $\sigma(\theta)$ values by **R-MTGB** model are visualized in Figure 3.

Table 4: Average MAE and RMSE scores, along with their standard deviations, computed by first averaging across all instances and tasks, then averaging over multiple runs for each evaluated model on both training and testing synthetic datasets. Best-performing values per dataset are indicated in boldface.

	MAE		RMSE	
	Train	Test	Train	Test
MTGB	0.265 ± 0.038	0.359 ± 0.048	0.340 ± 0.049	0.466 ± 0.061
DP-GB	0.444 ± 0.089	0.470 ± 0.091	0.583 ± 0.121	0.617 ± 0.125
R-MTGB	0.309 ± 0.041	$\mathbf{0.332 \pm 0.043}$	0.397 ± 0.053	$\mathbf{0.426 \pm 0.055}$
ST-GB	$\mathbf{0.260 \pm 0.044}$	0.365 ± 0.048	$\mathbf{0.333 \pm 0.056}$	0.472 ± 0.062
TaF-GB	0.387 ± 0.062	0.412 ± 0.065	0.504 ± 0.081	0.537 ± 0.085

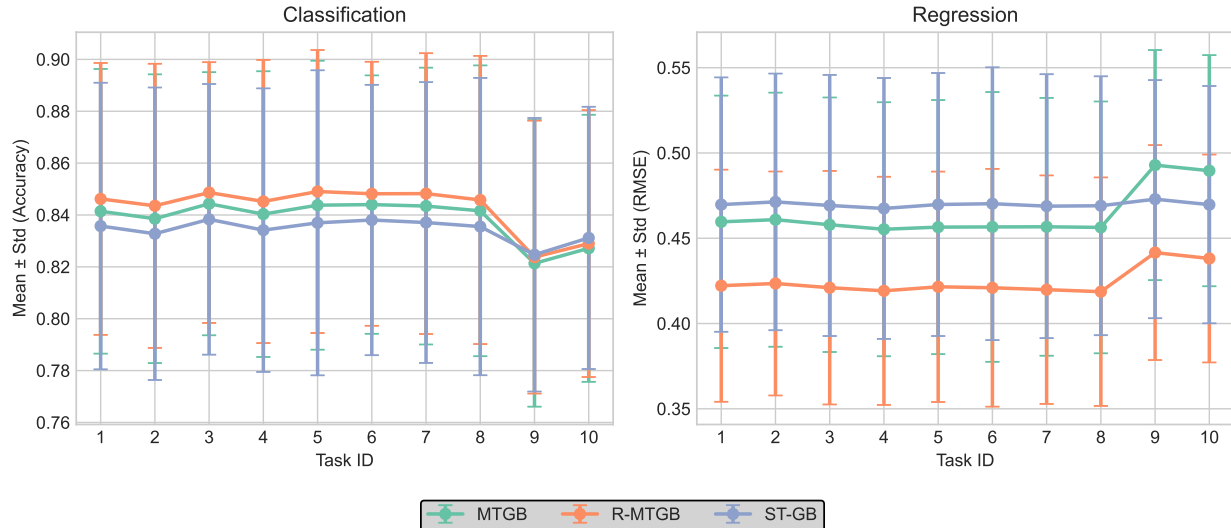


Figure 2: Average task-wise performance of the evaluated models over multiple runs, shown separately for classification (left subplot) and regression (right subplot) tasks.

The lines depict the mean values, while the shaded areas represent the corresponding standard deviations across multiple batches of experiments. Classification performance is shown as a solid line with light green shading, whereas regression performance is depicted with a dashed line and light orange shading. $\sigma(\theta)$ values should split tasks into outliers and non-outliers, but it is not clear which extreme values will be assigned to outlier or non-outlier tasks due to the random initialization of the θ values. The results demonstrate that **R-MTGB** model effectively identified outlier tasks by assigning them weights at the opposite extremes compared to common tasks. The small standard deviation observed across tasks, especially for the outliers, further highlights the robustness of the proposed parameter optimization.

4.4 Real-World Datasets Results

The experimental results of the evaluated models on real-world datasets (listed in Table 2) are summarized in Tables 5 through 8. All reported metrics are computed by first averaging across all instances and tasks within each batch, and then calculating the mean and standard deviation over 100 batch runs. Note that each dataset contains a different number of tasks. Specifically, Tables 5 and 6 present the average accuracy and unweighted mean recall on unseen test data for the classification datasets. Similarly, Tables 7 and 8 report the average RMSE and MAE on the test sets for the regression tasks. The best-performing results in each category are indicated in boldface for clarity.

The results in Table 5 clearly show that the proposed **R-MTGB** model consistently achieves the highest testing accuracy on all datasets, either matching or exceeding the performance of the competing methods. Notably, **R-MTGB** outperforms the other models on four out of five datasets and ties with **MTGB** on the *Landmine* dataset. As shown in Table 6, **R-MTGB** achieves the highest recall on three out of the five datasets: *Adult (Gender)*, *Adult (Race)*, and *Bank Marketing*, indicating strong overall performance across diverse classification tasks. **ST-GB** slightly outperforms **R-MTGB** on *Avila* and delivers the best result on *Landmine*, although the margin is small. In contrast, pooling-based approaches exhibit consistently lower recall and accuracy across all datasets, particularly on complex datasets such

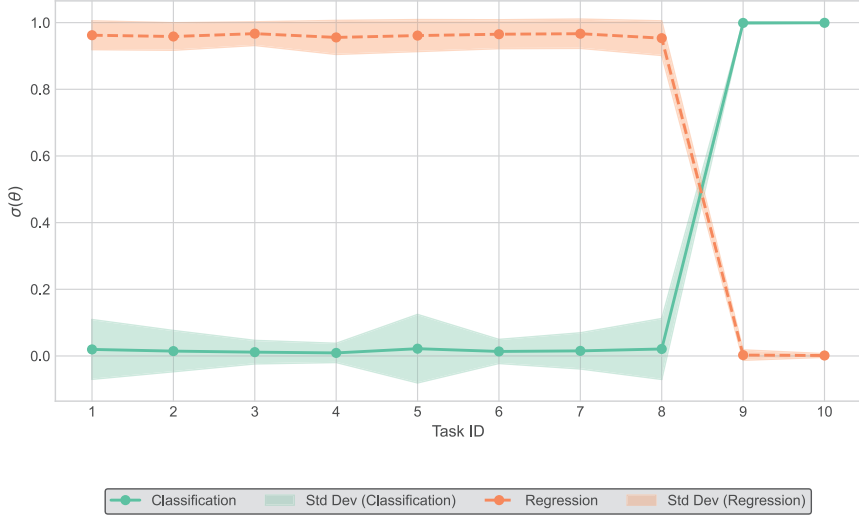


Figure 3: Mean and standard deviation of $\sigma(\theta)$ for each task learned by **R-MTGB** model on the generated synthetic multi-task data.

Table 5: Testing accuracy across studied models for each dataset. Results are first averaged over all instances and tasks within each batch, then reported as the mean and standard deviation across all runs. Best-performing values per dataset are indicated in boldface.

	Adult (Gender)	Adult (Race)	Avila	Bank Marketing	Landmine
MTGB	0.8479 ± 0.0036	0.8451 ± 0.0036	0.6138 ± 0.0503	0.8934 ± 0.0030	0.9428 ± 0.0035
DP-GB	0.8368 ± 0.0046	0.8368 ± 0.0046	0.4939 ± 0.0095	0.8889 ± 0.0029	0.9387 ± 0.0035
R-MTGB	0.8493 ± 0.0036	0.8487 ± 0.0036	0.6190 ± 0.0465	0.8947 ± 0.0031	0.9428 ± 0.0035
ST-GB	0.8406 ± 0.0036	0.8385 ± 0.0036	0.6099 ± 0.0605	0.8917 ± 0.0030	0.9423 ± 0.0035
TaF-GB	0.8368 ± 0.0046	0.8368 ± 0.0046	0.4970 ± 0.0090	0.8889 ± 0.0029	0.9387 ± 0.0035

as *Avila*. While **DP-GB** and **TaF-GB** perform moderately well, they do not surpass the top-performing methods on any dataset. Overall, these results further validate the effectiveness of **R-MTGB** in leveraging relational structure to enhance predictive performance across tasks.

Table 6: Testing recall across studied models for each dataset. Results are first averaged over all instances and tasks within each batch, then reported as the mean and standard deviation across all runs. Best-performing values per dataset are indicated in boldface.

	Adult (Gender)	Adult (Race)	Avila	Bank Marketing	Landmine
MTGB	0.7205 ± 0.0051	0.7158 ± 0.0080	0.4372 ± 0.0853	0.5765 ± 0.0099	0.5485 ± 0.0100
DP-GB	0.6838 ± 0.0099	0.6838 ± 0.0099	0.1660 ± 0.0083	0.5321 ± 0.0037	0.5 ± 0
R-MTGB	0.7256 ± 0.0057	0.7248 ± 0.0052	0.4360 ± 0.0832	0.5892 ± 0.0094	0.5478 ± 0.0099
ST-GB	0.7049 ± 0.0056	0.6931 ± 0.0083	0.4534 ± 0.0881	0.5552 ± 0.0050	0.5518 ± 0.0097
TaF-GB	0.6838 ± 0.0099	0.6838 ± 0.0099	0.1689 ± 0.0069	0.5321 ± 0.0037	0.5 ± 0

Regarding the regression datasets and **RMSE** metric (Table 7), **R-MTGB** achieves the lowest test errors on nearly all datasets, demonstrating remarkable effectiveness, especially on datasets with structurally complex tasks (e.g., *SARCOS*). **ST-GB**, while not the top performer overall, achieves the best results on the *Parkinsons* dataset with a trivial margin over **R-MTGB**. pooling-based methods like **DP-GB** generally underperform, especially on more complex datasets like *Parkinsons* and *SARCOS*. In terms of **MAE** results (Table 8), **R-MTGB** again demonstrates consistent superiority, achieving the lowest errors on the same datasets as those on **RMSE**, as shown in Table 7. **ST-GB** achieves the lowest **MAE** on *Parkinsons*, again with a minor difference compared to **R-MTGB**. As with the **RMSE** results,

Table 7: Testing RMSE across studied models for each dataset. Results are first averaged over all instances and tasks within each batch, then reported as the mean and standard deviation across all runs. Best-performing values per dataset are indicated in boldface.

	Abalone	Computer	Parkinson	SARCOS	School
MTGB	2.2894 ± 0.0866	2.4856 ± 0.0473	0.3355 ± 0.0243	4.8083 ± 0.0336	10.1536 ± 0.1222
DP-GB	2.3970 ± 0.0935	2.4658 ± 0.0478	8.8586 ± 0.1373	18.3971 ± 0.0669	10.4229 ± 0.1176
R-MTGB	2.2660 ± 0.0857	2.4632 ± 0.0706	0.2868 ± 0.0316	4.7031 ± 0.0729	10.1313 ± 0.1262
ST-GB	2.3464 ± 0.0889	2.7596 ± 0.3516	0.2684 ± 0.0274	4.9193 ± 0.0340	10.2952 ± 0.1366
TaF-GB	2.3830 ± 0.0926	2.4668 ± 0.0669	6.5588 ± 0.0871	11.2658 ± 0.0597	10.4152 ± 0.1166

pooling-based methods such as DP-GB lag behind, particularly on complex datasets like *Parkinsons* and *SARCOS*. These results confirm the overall trend that R-MTGB offers a competitive and efficient alternative, striking a balance between accuracy and scalability by capturing relational information across tasks in a single model. In comparison

Table 8: Testing MAE across studied models for each dataset. Results are first averaged over all instances and tasks within each batch, then reported as the mean and standard deviation across all runs. Best-performing values per dataset are indicated in boldface.

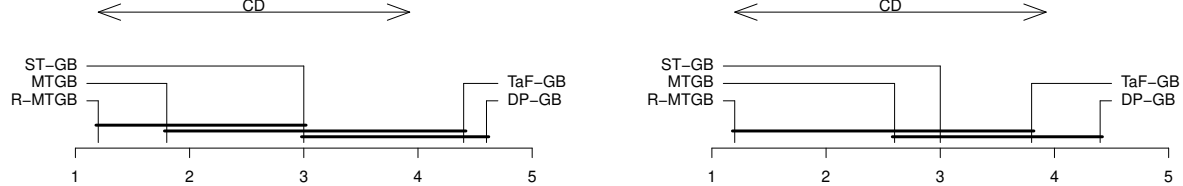
	Abalone	Computer	Parkinson	SARCOS	School
MTGB	1.6236 ± 0.0468	2.0536 ± 0.0437	0.1858 ± 0.0154	2.7778 ± 0.0156	8.0314 ± 0.0955
DP-GB	1.7322 ± 0.0502	2.0249 ± 0.0432	7.3403 ± 0.1180	12.6503 ± 0.0469	8.2701 ± 0.0975
R-MTGB	1.6073 ± 0.0459	2.0208 ± 0.0610	0.1315 ± 0.0253	2.7366 ± 0.0343	8.0048 ± 0.1018
ST-GB	1.6643 ± 0.0481	2.1966 ± 0.3169	0.1099 ± 0.0082	2.7783 ± 0.0154	8.1460 ± 0.1083
TaF-GB	1.7110 ± 0.0502	2.0430 ± 0.0556	5.7127 ± 0.0882	7.1316 ± 0.0305	8.2696 ± 0.0975

with the conventional MTGB model, the proposed R-MTGB consistently outperforms it across all metrics, tasks, and datasets. This demonstrates that the proposed approach effectively addresses the limitations of the conventional MTGB by incorporating a dynamic task reweighting mechanism.

To systematically compare model performance across datasets (dataset-wise) and tasks (task-wise), as shown in Figures 4 and 5, we employ Dems  r plots alongside the Nemenyi post-hoc test [77], using a significance level of $p = 0.05$. A Dems  r plot illustrates the average rank of each model across all evaluation scenarios. For each case, models are ranked based on performance, in descending order for classification (where higher accuracy is better) and in ascending order for regression (where lower RMSE is better). The top-performing model receives rank one, followed by rank two, and so on. These ranks are averaged across all scenarios, and further averaged over 100 independent experimental runs to yield a stable estimate of the average rank of each model. The Dems  r plot places each model along the horizontal axis according to this average rank, where models closer to the left have lower (better) ranks, indicating stronger overall performance. Finally, to determine whether differences between models are statistically significant, we apply the Nemenyi post-hoc test, which calculates Critical Distance (CD). If the average ranks of two models differ by more than the CD, their performance difference is considered statistically significant. In the plot, this is visualized using horizontal bars: models connected by a bar are not significantly different in performance.

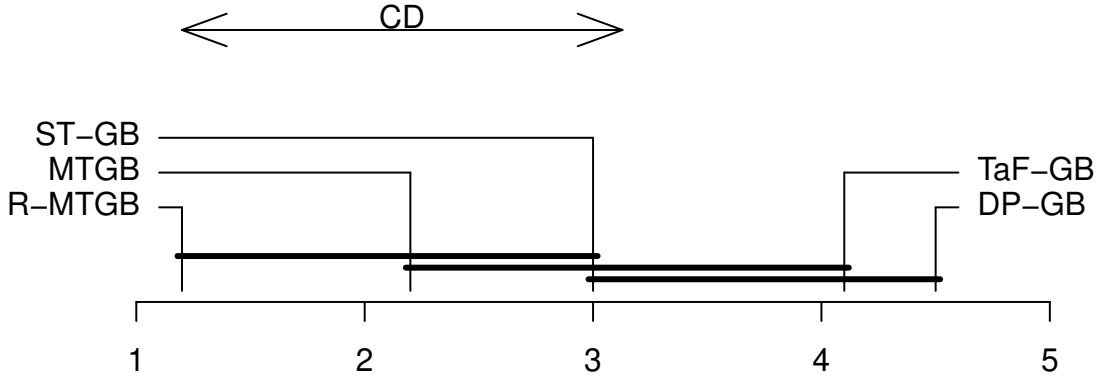
Our dataset-wise evaluation spans 10 datasets: 5 classification datasets (measured by accuracy) and 5 regression datasets (measured by RMSE) (see Figure 4). The resulting critical differences are approximately 2.72 for the classification and regression evaluations (Figure 4, subplots a and b), and 1.92 when considering all datasets jointly (Figure 4, subplot c). Figure 4 shows that R-MTGB model consistently achieves the lowest (best) average rank across all datasets and metrics. Although the differences between R-MTGB, conventional MTGB, and ST-GB models are not statistically significant across all comparisons, there is no significant difference between these models and TaF-GB specifically in regression tasks. Notably, R-MTGB maintains the best rank, followed by the conventional MTGB model, with a significant margin in regression and overall evaluations (subplots b and c). On the other hand, pooling-based models underperform relative to the others. These results underscore the advantages of the proposed robust MTL strategy compared to conventional and pooling-based approaches that indiscriminately combine task data.

For a more granular view, we conduct a task-wise comparison, applying the same statistical procedure to individual tasks. These evaluations consider only models capable of distinguishing between tasks, and compute average task-wise ranks over 100 runs to assess statistically significant performance differences. This analysis includes:



(a) Classification datasets

(b) Regression datasets



(c) All datasets

Figure 4: Demšar plots with Neményi test ($p = 0.05$) comparing model performance across datasets. The x-axis shows the average rank of each method over 100 runs; lower is better. Horizontal bars indicate methods with no significant difference. The CD for statistically significant differences is shown at the top.

- 96 classification tasks measured by accuracy, with a critical difference (CD) of approximately 0.33 (subplot a),
- 381 regression tasks measured by RMSE, with a CD of approximately 0.17 (subplot b), and
- a combined total of 477 tasks across all datasets, with a CD of approximately 0.15 (subplot c).

Figure 5, subplot (a), shows that **R-MTGB** model achieves the lowest (best) average rank. While there is no statistically significant difference between this model and the conventional **MTGB**, both outperform **ST-GB** model, although the difference is statistically significant. In the regression tasks presented in subplot (b), the proposed model again attains the best (lowest) average rank. Where the difference is statistically significant when compared to other approaches. Lastly, the overall task-wise ranking in subplot (c) indicates that the proposed model consistently achieves the top average rank across tasks, with statistically significant differences observed between **R-MTGB** other methodologies.

The consistently poor performance of **DP-GB** and **TaF-GB** across all scenarios in Figures 4 and 5 indicates that simple data aggregation can harm model effectiveness, likely due to the loss of task-specific distinctions and the introduction of noise. In contrast, the regularization mechanism in **R-MTGB** effectively leverages beneficial inter-task relationships while mitigating the negative effects of unrelated or noisy tasks, which is especially valuable in heterogeneous task

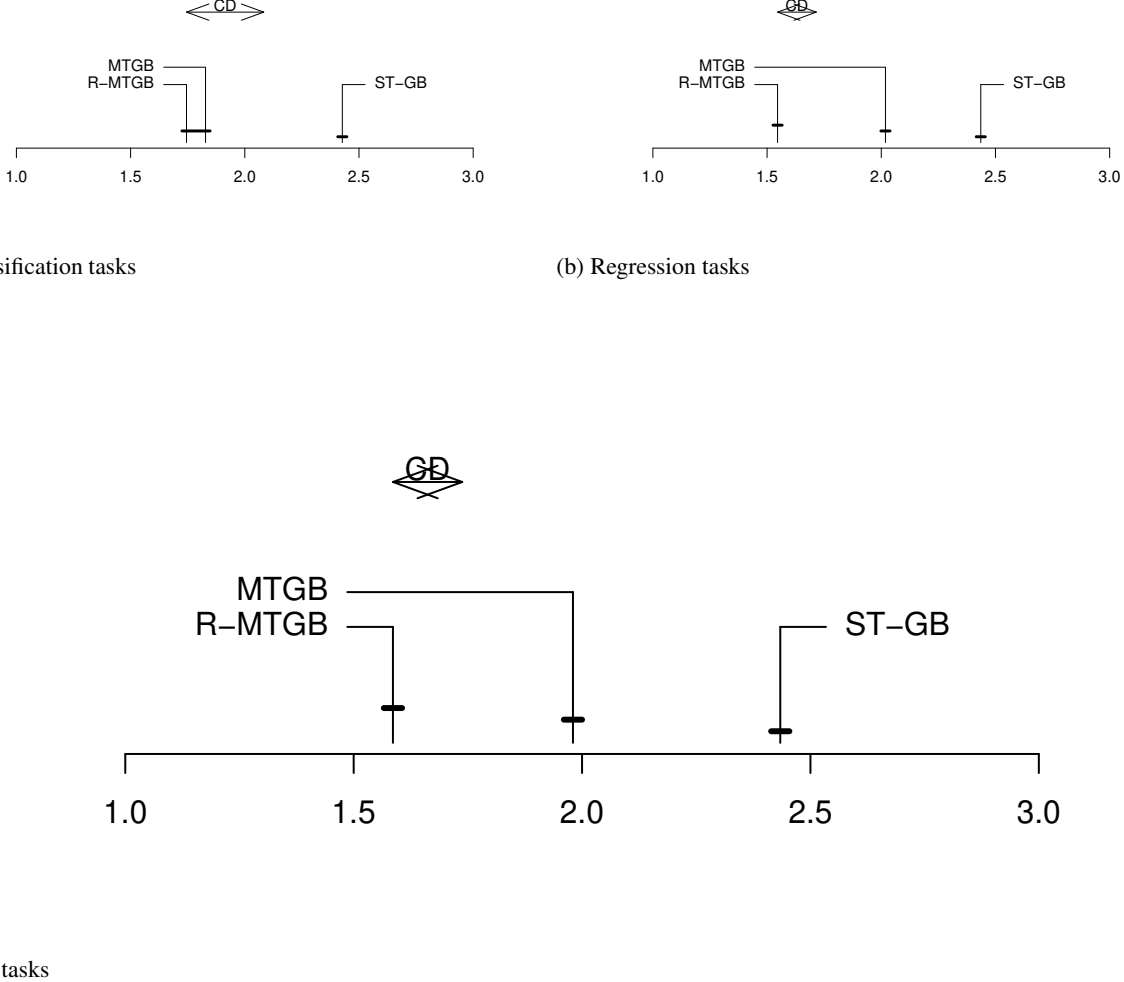


Figure 5: Demšar plots with Nemenyi test ($p = 0.05$) comparing model performance across tasks. The x-axis shows the average rank of each method over 100 runs; lower is better. Horizontal bars indicate methods with no significant difference. The **CD** for statistically significant differences is shown at the top.

environments. These findings highlight the effectiveness of **R-MTGB** approach, especially its capacity to identify and de-emphasize adversarial task. This makes it a compelling solution for **MTL** in both classification and regression scenarios across diverse datasets and tasks.

To evaluate the effectiveness of the proposed model in identifying outlier tasks, we analyzed the average optimized $\sigma(\theta)$ value for each task t across the experimental datasets. These $\sigma(\theta)$ values serve as task-specific outlier weights. After optimization, a value close to one indicates that the corresponding task is likely an outlier, whereas a value near zero suggests the task is likely an inlier or vice versa. Figure 6 shows the average learned θ vector parameter by **R-MTGB** model, across 100 runs for each dataset (subplots) alongside the standard deviation (shaded region) for each task. To ensure consistent directionality across different experiment runs, each vector $\sigma(\theta)$ is aligned with a reference vector (taken from the first run). Specifically, the first vector is stored as the reference. For each subsequent vector, the correlation with the reference is checked. If the correlation is negative—indicating opposite directionality—the vector is flipped by taking $1 - \sigma(\theta)$. This operation ensures that all vectors point in the same direction in the latent space, eliminating ambiguity due to symmetry. Moreover, consistent y-axis limits, enable direct comparison of $\sigma(\theta)$ magnitudes between analyzed datasets. For datasets containing distinguishable or noisy tasks, such as *Avila*, *School*, and *Bank Marketing*, **R-MTGB** consistently assigned $\sigma(\theta)$ values near the extremes, reflecting confident separation

between inlier and outlier tasks. In contrast, *Adults* datasets exhibit minimal variation in $\sigma(\theta)$ due to having fewer binary-sensitive attribute tasks, which resulted in more uniform or linearly distributed $\sigma(\theta)$ values. Moreover, the small or no standard deviation across tasks for complex datasets (e.g., *SARCOS*, *Avila*, and *Abalone*), indicates the robustness of the proposed model in identifying outlier tasks in various runs.

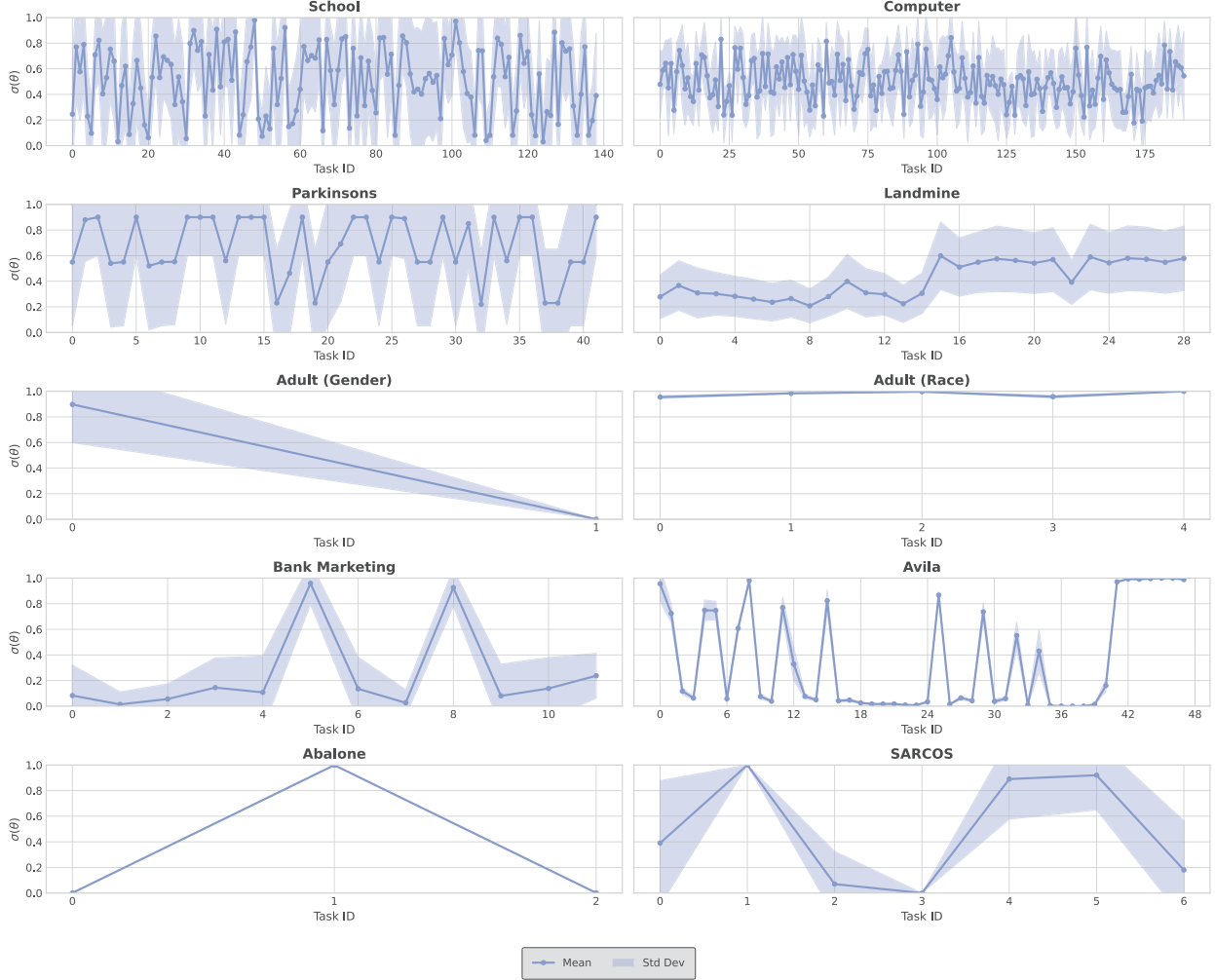


Figure 6: Mean and standard deviation of $\sigma(\theta)$ across multiple runs for each task learned by **R-MTGB** model, shown per dataset in the corresponding subplots.

5 Conclusions

In this study, we presented Robust-Multi-Task Gradient Boosting (**R-MTGB**) framework, a principled architecture composed of three blocks designed to address task heterogeneity in Multi-Task Learning (**MTL**). **R-MTGB** sequentially integrates shared-level knowledge, outlier-aware task partitioning, and task-specific fine-tuning, to build a composite prediction model that effectively balances generalization and specialization. Its ensemble-based formulation employs a learned, task-dependent weighting mechanism to adaptively interpolate between outlier and non-outlier behaviors, ensuring robust performance even in the presence of anomalous tasks. Notably, the model offers interpretability by revealing task-level outlier scores via the learned interpolation parameters, allowing for the diagnosis and visualization of tasks that significantly deviate from the shared structure.

Comprehensive experiments conducted on both synthetic and real-world datasets demonstrate the ability of the proposed model to generalize across tasks, maintain high predictive accuracy for each individual task, and robustly identify anomalous tasks. The results indicate that **R-MTGB** outperforms conventional Multi-Task Gradient Boost-

ing (**MTGB**), Single Task (**ST**) learning, and Data Pooling (**DP**) approaches, including augmented data pooling with task-specific information. Our experiments show that the advantages of the proposed method are more pronounced for regression tasks and comparatively smaller for classification tasks. These advantages hold across varying degrees of task heterogeneity, underscoring the robustness and adaptability of the proposed multi-task framework.

Declaration of Interests

The authors declare that there are no competing financial interests or personal relationships that could have potentially biased the research, experiments, or the conclusions presented in this manuscript.

Acknowledgments

The authors acknowledge financial support from the project PID2022-139856NB-I00, funded by MCIN/AEI/10.13039/501100011033/FEDER, UE; from project IDEA-CM (TEC-2024/COM-89), funded by the Autonomous Community of Madrid; and from the ELLIS Unit Madrid. The authors also acknowledge computational support from the Centro de Computación Científica-Universidad Autónoma de Madrid (CCC-UAM).

Data and Code Availability

The datasets utilized in this study were obtained from their respective publicly cited references. Both these datasets and the public source developed code for the proposed model are accessible at github.com/GAA-UAM/R-MTGB.

References

- [1] Yu Zhang and Qiang Yang. A survey on multi-task learning. *IEEE Transactions on Knowledge and Data Engineering*, 34(12):5586–5609, 2022.
- [2] Rich Caruana. Multitask learning. *Machine Learning*, 28(1):41–75, 1997.
- [3] Sheng Shen, Shijia Yang, Tianjun Zhang, Bohan Zhai, Joseph E. Gonzalez, Kurt Keutzer, and Trevor Darrell. Multitask vision-language prompt tuning. In *Proceedings of the IEEE/CVF Winter Conference on Applications of Computer Vision (WACV)*, pages 5656–5667, January 2024.
- [4] Tomáš Souček, Jean-Baptiste Alayrac, Antoine Miech, Ivan Laptev, and Josef Sivic. Multi-task learning of object states and state-modifying actions from web videos. *IEEE Transactions on Pattern Analysis and Machine Intelligence*, 46(7):5114–5130, 2024.
- [5] Qidong Liu, Xian Wu, Xiangyu Zhao, Yuanshao Zhu, Derong Xu, Feng Tian, and Yefeng Zheng. When moe meets llms: Parameter efficient fine-tuning for multi-task medical applications. In *Proceedings of the 47th International ACM SIGIR Conference on Research and Development in Information Retrieval*, pages 1104–1114. Association for Computing Machinery, 2024.
- [6] Hsinhan Tsai, Ta-Wei Yang, Tien-Yi Wu, Ya-Chi Tu, Cheng-Lung Chen, and Cheng-Fu Chou. Multitask learning multimodal network for chronic disease prediction. *Scientific Reports*, 15(1):15468, 2025.
- [7] Shipeng Yu, Volker Tresp, and Kai Yu. Robust multi-task learning with t-processes. In *Proceedings of the 24th International Conference on Machine Learning*, pages 1103–1110. Association for Computing Machinery, 2007.
- [8] Tianqi Chen and Carlos Guestrin. Xgboost: A scalable tree boosting system. In *Proceedings of the 22nd ACM SIGKDD International Conference on Knowledge Discovery and Data Mining*, pages 785–794. Association for Computing Machinery, 2016.
- [9] Candice Bentéjac, Anna Csörgő, and Gonzalo Martínez-Muñoz. A comparative analysis of gradient boosting algorithms. *Artificial Intelligence Review*, 54(3):1937–1967, 2021.
- [10] Ravid Shwartz-Ziv and Amitai Armon. Tabular data: Deep learning is not all you need. *Information Fusion*, 81:84–90, 2022.
- [11] Olivier Chapelle, Pannagadatta Shivaswamy, Srinivas Vadrevu, Kilian Weinberger, Ya Zhang, and Belle Tseng. Boosted multi-task learning. *Machine Learning*, 85(1-2):149–173, Oct 2011.
- [12] Seyedamani Emami, Carlos Ruiz Pastor, and Gonzalo Martínez-Muñoz. Multi-task gradient boosting. In *Hybrid Artificial Intelligent Systems*, pages 97–107, Cham, 2023. Springer Nature Switzerland.

[13] Yu Zhang and Dit-Yan Yeung. Multi-task boosting by exploiting task relationships. In Peter A. Flach, Tijl De Bie, and Nello Cristianini, editors, *Machine Learning and Knowledge Discovery in Databases*, pages 697–710. Springer Berlin Heidelberg, 2012.

[14] Alexis Bellot and Mihaela van der Schaar. Multitask boosting for survival analysis with competing risks. In *Advances in Neural Information Processing Systems*, volume 31. Curran Associates, Inc., 2018.

[15] Pinghua Gong, Jieping Ye, and Changshui Zhang. Robust multi-task feature learning. In *Proceedings of the 18th ACM SIGKDD international conference on Knowledge discovery and data mining*, pages 895–903, 2012.

[16] Isabelle Leang, Ganesh Sistu, Fabian Bürger, Andrei Bursuc, and Senthil Yogamani. Dynamic task weighting methods for multi-task networks in autonomous driving systems. In *2020 IEEE 23rd International Conference on Intelligent Transportation Systems (ITSC)*, pages 1–8, 2020.

[17] Ya Li, Xinmei Tian, Tongliang Liu, and Dacheng Tao. Multi-task model and feature joint learning. In *IJCAI*, pages 3643–3649, 2015.

[18] Xuejun Liao and Lawrence Carin. Radial basis function network for multi-task learning. In *Advances in Neural Information Processing Systems*, volume 18. MIT Press, 2005.

[19] Zhanpeng Zhang, Ping Luo, Chen Change Loy, and Xiaoou Tang. Facial landmark detection by deep multi-task learning. In *Computer Vision – ECCV 2014*, pages 94–108, Cham, 2014. Springer International Publishing.

[20] Sijin LI, Zhi-Qiang Liu, and Antoni B. Chan. Heterogeneous multi-task learning for human pose estimation with deep convolutional neural network. In *Proceedings of the IEEE Conference on Computer Vision and Pattern Recognition (CVPR) Workshops*, pages 482–489, June 2014.

[21] Wu Liu, Tao Mei, Yongdong Zhang, Cherry Che, and Jiebo Luo. Multi-task deep visual-semantic embedding for video thumbnail selection. In *Proceedings of the IEEE Conference on Computer Vision and Pattern Recognition (CVPR)*, pages 3707–3715, June 2015.

[22] Wenlu Zhang, Rongjian Li, Tao Zeng, Qian Sun, Sudhir Kumar, Jieping Ye, and Shuiwang Ji. Deep model based transfer and multi-task learning for biological image analysis. In *Proceedings of the 21th ACM SIGKDD International Conference on Knowledge Discovery and Data Mining*, pages 1475–1484. Association for Computing Machinery, 2015.

[23] Rie Kubota Ando, Tong Zhang, and Peter Bartlett. A framework for learning predictive structures from multiple tasks and unlabeled data. *Journal of machine learning research*, 6(11), 2005.

[24] Ahmed Agiza, Marina Neseem, and Sherief Reda. Mtlora: Low-rank adaptation approach for efficient multi-task learning. In *Proceedings of the IEEE/CVF Conference on Computer Vision and Pattern Recognition (CVPR)*, pages 16196–16205, June 2024.

[25] Jianhui Chen, Jiayu Zhou, and Jieping Ye. Integrating low-rank and group-sparse structures for robust multi-task learning. In *Proceedings of the 17th ACM SIGKDD International Conference on Knowledge Discovery and Data Mining*, pages 42–50. Association for Computing Machinery, 2011.

[26] Lei Han and Yu Zhang. Multi-stage multi-task learning with reduced rank. *Proceedings of the AAAI Conference on Artificial Intelligence*, 30(1), Feb. 2016.

[27] Sebastian Thrun and Joseph O’Sullivan. Discovering structure in multiple learning tasks: The tc algorithm. In *ICML*, volume 96, pages 489–497. Citeseer, 1996.

[28] Koby Crammer and Yishay Mansour. Learning multiple tasks using shared hypotheses. In F. Pereira, C.J. Burges, L. Bottou, and K.Q. Weinberger, editors, *Advances in Neural Information Processing Systems*, volume 25. Curran Associates, Inc., 2012.

[29] Theodoros Evgeniou and Massimiliano Pontil. Regularized multi-task learning. In *Proceedings of the Tenth ACM SIGKDD International Conference on Knowledge Discovery and Data Mining*, pages 109–117. Association for Computing Machinery, 2004.

[30] Shabin Parameswaran and Kilian Q Weinberger. Large margin multi-task metric learning. In *Advances in Neural Information Processing Systems*, volume 23. Curran Associates, Inc., 2010.

[31] Theodoros Evgeniou, Charles A Micchelli, Massimiliano Pontil, and John Shawe-Taylor. Learning multiple tasks with kernel methods. *Journal of machine learning research*, 6(4), 2005.

[32] Tsuyoshi Kato, Hisashi Kashima, Masashi Sugiyama, and Kiyoshi Asai. Multi-task learning via conic programming. In *Advances in Neural Information Processing Systems*, volume 20. Curran Associates, Inc., 2007.

[33] Lei Han and Yu Zhang. Learning tree structure in multi-task learning. In *Proceedings of the 21th ACM SIGKDD International Conference on Knowledge Discovery and Data Mining*, pages 397–406. Association for Computing Machinery, 2015.

[34] Balaji Lakshminarayanan, Alexander Pritzel, and Charles Blundell. Simple and scalable predictive uncertainty estimation using deep ensembles. In *Advances in Neural Information Processing Systems*, volume 30. Curran Associates, Inc., 2017.

[35] Guoxuan Xia and Christos-Savvas Bouganis. Window-based early-exit cascades for uncertainty estimation: When deep ensembles are more efficient than single models. In *Proceedings of the IEEE/CVF International Conference on Computer Vision (ICCV)*, pages 17368–17380, October 2023.

[36] Zhi-Hua Zhou. Ensemble methods: Foundations and algorithms. 2012.

[37] Jerome H. Friedman. Greedy function approximation: A gradient boosting machine. *The Annals of Statistics*, 29(5):1189–1232, 2001.

[38] Guolin Ke, Qi Meng, Thomas Finley, Taifeng Wang, Wei Chen, Weidong Ma, Qiwei Ye, and Tie-Yan Liu. Lightgbm: A highly efficient gradient boosting decision tree. In *Advances in Neural Information Processing Systems*, volume 30. Curran Associates, Inc., 2017.

[39] Liudmila Prokhorenkova, Gleb Gusev, Aleksandr Vorobev, Anna Veronika Dorogush, and Andrey Gulin. Catboost: unbiased boosting with categorical features. In *Advances in Neural Information Processing Systems*, volume 31. Curran Associates, Inc., 2018.

[40] Zhendong Zhang and Cheolkon Jung. Gbdt-mo: Gradient-boosted decision trees for multiple outputs. *IEEE Transactions on Neural Networks and Learning Systems*, 32(7):3156–3167, 2021.

[41] Seyedamani Emami and Gonzalo Martínez-Muñoz. Condensed-gradient boosting. *International Journal of Machine Learning and Cybernetics*, 16(1):687–701, 2025.

[42] Jian Jiang, Rui Wang, Menglun Wang, Kaifu Gao, Duc Duy Nguyen, and Guo-Wei Wei. Boosting tree-assisted multitask deep learning for small scientific datasets. *Journal of chemical information and modeling*, 60(3):1235–1244, 2020.

[43] Haizhou Liu, Xuan Zhang, Hongbin Sun, and Mohammad Shahidehpour. Boosted multi-task learning for inter-district collaborative load forecasting. *IEEE Transactions on Smart Grid*, 15(1):973–986, 2024.

[44] Mingcheng Chen, Zhenghui Wang, Zhiyun Zhao, Weinan Zhang, Xiawei Guo, Jian Shen, Yanru Qu, Jieli Lu, Min Xu, Yu Xu, Tiange Wang, Mian Li, Weiwei Tu, Yong Yu, Yufang Bi, Weiqing Wang, and Guang Ning. Task-wise split gradient boosting trees for multi-center diabetes prediction. In *Proceedings of the 27th ACM SIGKDD Conference on Knowledge Discovery & Data Mining*, pages 2663–2673, 2021.

[45] Handong Ma, Zhecheng Dong, Mingcheng Chen, Wenbo Sheng, Yao Li, Weinan Zhang, Shaodian Zhang, and Yong Yu. A gradient boosting tree model for multi-department venous thromboembolism risk assessment with imbalanced data. *Journal of Biomedical Informatics*, 134:104210, 2022.

[46] ZhenZhe Ying, Zhuoer Xu, Zhifeng Li, Weiqiang Wang, and Changhua Meng. Mt-gbm: A multi-task gradient boosting machine with shared decision trees, 2022.

[47] Samir Touzani, Jessica Granderson, and Samuel Fernandes. Gradient boosting machine for modeling the energy consumption of commercial buildings. *Energy and Buildings*, 158:1533–1543, 2018.

[48] Wenchao Zhang, Peixin Shi, Pengjiao Jia, and Xiaoqi Zhou. A novel gradient boosting approach for imbalanced regression. *Neurocomputing*, 601:128091, 2024.

[49] Altyeb Altaher Taha and Sharaf Jameel Malebary. An intelligent approach to credit card fraud detection using an optimized light gradient boosting machine. *IEEE Access*, 8:25579–25587, 2020.

[50] Nuwan Gunasekara, Bernhard Pfahringer, Heitor Gomes, and Albert Bifet. Gradient boosted trees for evolving data streams. *Machine Learning*, 113(5):3325–3352, may 2024.

[51] Antonella Plaia, Simona Buscemi, Johannes Fürnkranz, and Eneldo Loza Mencía. Comparing boosting and bagging for decision trees of rankings. *Journal of Classification*, 39(1):78–99, 2022.

[52] Manar D. Samad, Sakib Abrar, and Norou Diawara. Missing value estimation using clustering and deep learning within multiple imputation framework. *Knowledge-Based Systems*, 249:108968, 2022.

[53] Alexey Natekin and Alois Knoll. Gradient boosting machines, a tutorial. *Frontiers in Neurorobotics*, Volume 7 - 2013, 2013.

[54] Fabian Pedregosa, Gaël Varoquaux, Alexandre Gramfort, Vincent Michel, Bertrand Thirion, Olivier Grisel, Mathieu Blondel, Peter Prettenhofer, Ron Weiss, Vincent Dubourg, et al. Scikit-learn: Machine learning in python. *the Journal of machine Learning research*, 12:2825–2830, 2011.

[55] C. De Stefano, M. Maniaci, F. Fontanella, and A. Scotto di Freca. Reliable writer identification in medieval manuscripts through page layout features: The “avila” bible case. *Engineering Applications of Artificial Intelligence*, 72:99–110, 2018.

[56] Barry Becker and Ronny Kohavi. Adult, 1996. UCI Machine Learning Repository.

[57] Luca Oneto, Michele Doninini, Amon Elders, and Massimiliano Pontil. Taking advantage of multitask learning for fair classification. In *Proceedings of the 2019 AAAI/ACM Conference on AI, Ethics, and Society*, pages 227–237. Association for Computing Machinery, 2019.

[58] Yuyan Wang, Xuezhi Wang, Alex Beutel, Flavien Prost, Jilin Chen, and Ed H. Chi. Understanding and improving fairness-accuracy trade-offs in multi-task learning. In *Proceedings of the 27th ACM SIGKDD Conference on Knowledge Discovery & Data Mining*, pages 1748–1757. Association for Computing Machinery, 2021.

[59] S. Moro, R. Laureano, and P. Cortez. Using data mining for bank direct marketing: An application of the crisp-dm methodology. In *Proceedings of the European Simulation and Modelling Conference - ESM'2011*, pages 117–121. EUROSIS, October 2011.

[60] Cemal Yilmaz, Hamdi Tolga Kahraman, and Salih Söyler. Passive mine detection and classification method based on hybrid model. *IEEE Access*, 6:47870–47888, 2018.

[61] Mengchen Zhao, Bo An, Yaodong Yu, Sulin Liu, and Sinno Pan. Data poisoning attacks on multi-task relationship learning. *Proceedings of the AAAI Conference on Artificial Intelligence*, 32(1), Apr. 2018.

[62] Warwick Nash, Tracy Sellers, Simon Talbot, Andrew Cawthorn, and Wes Ford. Abalone. UCI Machine Learning Repository, 1994.

[63] Carlos Ruiz, Carlos M. Alaíz, and José R. Dorronsoro. A convex formulation of svm-based multi-task learning. In *Hybrid Artificial Intelligent Systems*, pages 404–415, Cham, 2019. Springer International Publishing.

[64] Jintao Huang, Chuangquan Chen, Chi-Man Vong, and Yiu-Ming Cheung. Broad multitask learning system with group sparse regularization. *IEEE Transactions on Neural Networks and Learning Systems*, 36(5):8265–8278, 2025.

[65] Peter J. Lenk, Wayne S. DeSarbo, Paul E. Green, and Martin R. Young. Hierarchical bayes conjoint analysis: Recovery of partworth heterogeneity from reduced experimental designs. *Marketing Science*, 15(2):173–191, 1996.

[66] Andreas Argyriou, Massimiliano Pontil, Yiming Ying, and Charles Micchelli. A spectral regularization framework for multi-task structure learning. In *Advances in Neural Information Processing Systems*, volume 20. Curran Associates, Inc., 2007.

[67] Andreas Argyriou, Theodoros Evgeniou, and Massimiliano Pontil. Convex multi-task feature learning. *Machine Learning*, 73(3):243–272, 2008.

[68] Athanasios Tsanas and Max Little. Parkinsons Telemonitoring. UCI Machine Learning Repository, 2009.

[69] Hakan Gunduz. Deep learning-based parkinson’s disease classification using vocal feature sets. *IEEE Access*, 7:115540–115551, 2019.

[70] Saravanan Srinivasan, Parthasarathy Ramadass, Sandeep Kumar Mathivanan, Karthikeyan Panneer Selvam, Basu Dev Shrivahare, and Mohd Asif Shah. Detection of parkinson disease using multiclass machine learning approach. *Scientific Reports*, 14(1):13813, 2024.

[71] Pratik Kumar Jawanpuria, Maksim Lapin, Matthias Hein, and Bernt Schiele. Efficient output kernel learning for multiple tasks. In *Advances in Neural Information Processing Systems*, volume 28. Curran Associates, Inc., 2015.

[72] Jiejie Zhao, Bowen Du, Leilei Sun, Fuzhen Zhuang, Weifeng Lv, and Hui Xiong. Multiple relational attention network for multi-task learning. In *Proceedings of the 25th ACM SIGKDD International Conference on Knowledge Discovery & Data Mining*, pages 1123–1131, New York, NY, USA, 2019. Association for Computing Machinery.

[73] Carlo Ciliberto, Alessandro Rudi, Lorenzo Rosasco, and Massimiliano Pontil. Consistent multitask learning with nonlinear output relations. In *Advances in Neural Information Processing Systems*, volume 30. Curran Associates, Inc., 2017.

[74] Sinan Wang, Yumeng Li, Hongyan Li, Tanchao Zhu, Zhao Li, and Wenwu Ou. Multi-task learning with calibrated mixture of insightful experts. In *2022 IEEE 38th International Conference on Data Engineering (ICDE)*, pages 3307–3319, 2022.

[75] Bart Bakker and Tom Heskes. Task clustering and gating for bayesian multitask learning. *Journal of Machine Learning Research*, 4(May):83–99, 2003.

- [76] Ali Rahimi and Benjamin Recht. Random features for large-scale kernel machines. In *Advances in Neural Information Processing Systems*, volume 20. Curran Associates, Inc., 2007.
- [77] Janez Demšar. Statistical comparisons of classifiers over multiple data sets. *The Journal of Machine Learning Research*, 7:1–30, 2006.